1974

An objective technique for estimating large-scale flow pattern in the tropical upper troposphere from digitized cloud brightness data.

Jacobs, Frederick T.

Monterey, California. Naval Postgraduate School

AN OBJECTIVE TECHNIQUE FOR ESTIMATING LARGE-SCALE FLOW PATTERN IN THE TROPICAL UPPER TROPOSPHERE FROM DIGITIZED CLOUD BRIGHTNESS DATA

Frederick T. Jacobs

NAVAL POSTGRADUATE SCHOOL
Monterey, California

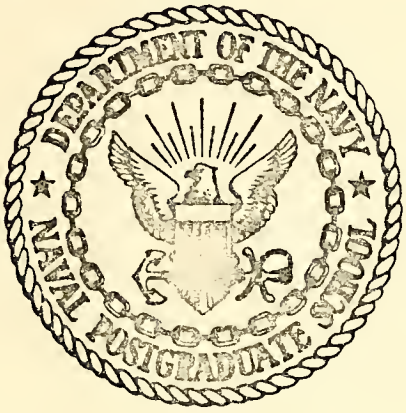

THESIS

AN OBJECTIVE TECHNIQUE FOR ESTIMATING LARGE-SCALE FLOW PATTERN IN THE TROPICAL UPPER TROPOSPHERE FROM DIGITIZED CLOUD BRIGHTNESS DATA

by

Frederick T. Jacobs

September 1974

Thesis Advisor: C.-P. Chang

Approved for public release; distribution unlimited.

SECURITY CLASSIFICATION OF THIS PAGE (When Data Entered)

REPORT DOCUMENTATION PAGE

READ INSTRUCTIONS BEFORE COMPLETING FORM

1. REPORT NUMBER

2. GOVT ACCESSION NO.

3. RECIPIENT'S CATALOG NUMBER

4. TITLE (and Subtitle)

An Objective Technique for Estimating Large-Scale Flow Pattern in the Tropical Upper Troposphere from Digitized Cloud Brightness Data

5. TYPE OF REPORT & PERIOD COVERED

Master's Thesis
September 1974

6. PERFORMING ORG. REPORT NUMBER

7. AUTHOR(s)

Frederick T. Jacobs

8. CONTRACT OR GRANT NUMBER(s)

9. PERFORMING ORGANIZATION NAME AND ADDRESS

Naval Postgraduate School
Monterey, California 93940

10. PROGRAM ELEMENT, PROJECT, TASK AREA & WORK UNIT NUMBERS

11. CONTROLLING OFFICE NAME AND ADDRESS

Naval Postgraduate School
Monterey, California

12. REPORT DATE

September 1974

13. NUMBER OF PAGES

60

14. MONITORING AGENCY NAME & ADDRESS(if different from Controlling Office)

Naval Postgraduate School
Monterey, California 93940

15. SECURITY CLASS. (of this report)

Unclassified

15a. DECLASSIFICATION/DOWNGRADING SCHEDULE

16. DISTRIBUTION STATEMENT (of this Report)

Approved for public release; distribution unlimited.

17. DISTRIBUTION STATEMENT (of the abstract entered in Block 20, if different from Report)

18. SUPPLEMENTARY NOTES

19. KEY WORDS (Continue on reverse side if necessary and identify by block number)

Objective technique
Tropical upper tropospheric analysis
Satellite brightness data
Equivalent divergence forcing

20. ABSTRACT (Continue on reverse side if necessary and identify by block number)

An objective technique is proposed to use digitized satellite cloud brightness data to estimate large-scale flow patterns over data-void tropical regions. It is basically a diagnostic model which assumes: 1) area-averaged cloud brightness is positively correlated with large-scale divergence in the tropical upper troposphere; and 2) large-scale tropical flow is quasi-barotropic and quasi-non-divergent. It can be used at any upper level where divergence is important in determining vorticity. The model requires:

DD FORM 1 JAN 73 1473 EDITION OF 1 NOV 65 IS OBSOLETE
S/N 0102-014-6601 |
(Page 1)

SECURITY CLASSIFICATION OF THIS PAGE (When Data Entered)

1) boundary conditions determined from surrounding wind reports, 2) a mean zonal flow determined from climatology, and 3) an equivalent divergence forcing function constructed empirically from the brightness data.

The technique is tested daily over a western North Pacific region for July-August 1971. Results show that for 25% of the days tested, the model produces a flow field which accurately resembles the major features of the stream-function field analyzed by NMC. In another 30% of the days it provides some valuable information about the flow patterns which would be difficult to obtain from boundary information alone. Experiments also suggest that improvement of the model may be made when satellite infrared data is available.

An Objective Technique for Estimating Large-Scale Flow Pattern in the Tropical Upper Troposphere from Digitized Cloud Brightness Data

by

Frederick T. Jacobs
Lieutenant, United States Navy
B.A., Miami University, 1967

Submitted in partial fulfillment of the
requirements for the degree of

MASTER OF SCIENCE IN METEOROLOGY

from the

NAVAL POSTGRADUATE SCHOOL
September 1974

ABSTRACT

An objective technique is proposed to use digitized satellite cloud brightness data to estimate large-scale flow patterns over data-void tropical regions. It is basically a diagnostic model which assumes: 1) area-averaged cloud brightness is positively correlated with large-scale divergence in the tropical upper troposphere; and 2) large-scale tropical flow is quasi-barotropic and quasi-non-divergent. It can be used at any upper level where divergence is important in determining vorticity. The model requires: 1) boundary conditions determined from surrounding wind reports, 2) a mean zonal flow determined from climatology, and 3) an equivalent divergence forcing function constructed empirically from the brightness data.

The technique is tested daily over a western North Pacific region for July-August 1971. Results show that for 25% of the days tested, the model produces a flow field which accurately resembles the major features of the stream-function field analyzed by NMC. In another 30% of the days it provides some valuable information about the flow patterns which would be difficult to obtain from boundary information alone. Experiments also suggest that improvement of the model may be made when satellite infrared data is available.

TABLE OF CONTENTS

LIST OF FIGURES

ACKNOWLEDGMENT

The author wishes to express his appreciation to Professor C.-P. Chang, for his advice and guidance throughout this study, to Mr. Steve Rinard and LCDR Eriberto Varona for their assistance in data reduction, and to Professor G. J. Haltiner for reading the manuscript. The satellite brightness and tropical grid data used in this study were provided by Mr. Roy Jenne of the National Center for Atmospheric Research. The satellite infrared data was provided by Dr. Jay S. Winston of the Meteorological Satellite Laboratory. All computations were made at the W. R. Church Computer Center of the Naval Postgraduate School. The research was partially supported by the National Environmental Satellite Service, National Oceanic and Atmospheric Administration, under contract NA-833-73, and by Fleet Numerical Weather Central.

I. INTRODUCTION

Satellite photographs of tropical regions have revealed that much of the tropical cloudiness is in the form of large, connected masses of very bright clouds. These masses are composed of many individual cumulus clouds, whose extensive cirrus canopies with a horizontal scale of several hundred km or larger account for most of their brightness. These large, bright cloud masses, or "cloud clusters" as they are now called, have received considerable attention in recent years. Chang (1970) and Wallace (1970, 1971), using time-longitude series of satellite photographs, found that many cloud clusters over the tropical Pacific are well organized and have characteristics resembling those of synoptic-scale westward propagating wave disturbances. Further evidence by Reed and Recker (1971) showed that these propagating cloud clusters in the western North Pacific are linked to synoptic-scale waves in the wind fields. Williams and Gray (1973) and Yanai et al (1973) have also deduced the mean properties of these western North Pacific cloud clusters and found several vertical characteristics of the active clusters similar to those found by Reed and Recker (1971) and Nitta (1972) for the wave troughs.

Due to the poor radiosonde coverage over the vast tropical oceans, it is natural to try to utilize the available satellite data as an aid for tropical analysis. Digitized cloud brightness data, acquired by the Advanced Vidicon Camera System of the operational satellite system have been available since 1967. Because of the relationship

between the bright cloud clusters and synoptic-scale tropical motions, this data becomes a potential source for such a purpose. In fact, evidences of relations between the satellite brightness data and other meteorological parameters have been found by several investigators. The correlation between brightness and precipitation has led to many attempts to estimate rainfall using satellite brightness [for example, see review by Martin and Scherer (1973)]. Wallace (1971) also found indication of good correspondence between area-averaged cloud brightness and synoptic-scale vertical motion associated with the 4- to 5-day tropical disturbances in the Kwajalein-Eniwetok-Ponape triangle of the Marshall Islands and the Guam-Truk-Yap triangle further west. He postulated that it may be possible to obtain an estimate of the vertical motion field over the tropics from the cloud brightness data alone. If this turns out to be the case, the satellite cloud brightness data will certainly be one of the best available indicators of disturbed weather in the tropics.

There are physical reasons to think that brightness data is closely related to the large-scale vertical motion field. The bright cirrus canopies associated with the cloud clusters "are produced by outflow from and remnants of cumulonimbi. In general, developing and conservative clusters maintain their cumulonimbi from a steady low-level mass convergence; clusters gradually die when their low-level mass convergence is eliminated" (Williams and Gray, 1973). Because of the readily available low-level moisture, the large-scale upward motion provides a favorable environment for the development and existence of the clusters. Furthermore, brighter clouds are usually thicker and therefore may

indicate larger amount of latent heat release (Gruber, 1974). Because the magnitude of the latent heating is nearly one order greater than the temperature fluctuations at most levels for large-scale, convectively-active tropical motions, thermal energy balance requires that the large-scale vertical motion must be approximately proportional to heating (Wallace, 1971; Holton, 1972). Thus one could expect a positive correlation between cloud brightness and large-scale vertical motion by reason of heating alone.

The correspondence between brightness and vertical motion may also be extended to large-scale horizontal divergence at levels where divergence is large, since many observational studies [Wallace (1971), Reed and Recker (1971), Nitta (1972), Williams and Gray (1973), Yanai et al (1973), Reed and Johnson (1974)] have produced very similar profiles of the vertical motion (or divergence) over tropical areas where covection is active. The same conclusion can also be inferred from the various vertical heating profiles shown by Hayashi (1974) from analyses of tropical output from the general circulation model of the NOAA Geophysical Fluid Dynamics Laboratory at Princeton. In addition, Williams and Gray (1973) have shown a clear in-phase relation between cloud clusters and upper-level divergence in their composite study.

So far, the use of satellite brightness data as an aid to tropical analysis has been limited to subjective methods only; i.e., an analyst relying on visual inspection of the satellite photographs to modify conventional weather maps. If the digitized brightness data can be used to estimate the large-scale vertical motion, as postulated by Wallace, and upper-level divergence, as reasoned above, then there may be ways

to use this digitized data in an objective manner. The purpose of this study is to propose such a technique in which the digitized brightness will be used to objectively diagnose the large-scale flow pattern in the tropical upper troposphere over regions where wind reports are sparse or void.

In Section II, the design of the objective technique, which is essentially a barotropic diagnostic model based on several observed properties of the large-scale tropical motions, will be discussed. In Section III the data used in the experiments of the technique will be described. The results of these experiments will be presented in Section IV.

II. DESIGN OF THE BASIC MODEL

The objective technique of using digitized satellite cloud brightness to diagnose large-scale tropical flow is based on two primary suppositions:

1) Brightness is positively correlated with active convection, and therefore with large-scale condensation heating, vertical motion and upper-level divergence.

2) Large-scale tropical flow is usually quasi-barotropic and quasi-non-divergent.

The model used is essentially a linearized barotropic vorticity equation which may be applied at any level where divergence is relatively important in determining the rotational part of the flow, such as the maximum-divergence level or the "outflow" level of the cloud clusters which is usually near 200-mb in the tropics. It is similar to the simple diagnostic model by Holton and Colton (1972) for the 200-mb seasonal mean circulations during the northern summer, in which the mean motion field was successfully reproduced by the steady-state solution of a linearized barotropic vorticity equation with observed mean divergence and mean zonal wind. In our model the vorticity equation is applied to a data-void region on a daily basis, with horizontal divergence replaced by an "equivalent divergence" field derived from the brightness data, basic zonal wind given by climatology, and boundary conditions determined by the data-rich surrounding areas. Similar to Holton and Colton's time-mean model, a damping coefficient is introduced to parameterize the

strong damping process in the tropical upper troposphere as reported by several vorticity budget studies (Reed and Recker, 1971; Williams and Gray, 1973; and others). We hope this model can reasonably describe the rotational part of the large-scale motion near the outflow level, and it may be useful for diagnostic purposes if we know what kind of solution can best approximate the actual motion field. If 12-hr or 24-hr history is available (presumably by use of this technique at an earlier time or by some other means), extrapolation in time may be used. However, the previous vorticity budget studies have consistently shown that the local change of vorticity near the maximum-divergence level is rather small when compared to other terms in the vorticity equation, thus a diagnosis of the flow at this level over the data-void region may be obtained by way of a steady-state solution of the vorticity equation. We hope that this solution may, to some degree, resemble the actual flow pattern and can be useful for large-scale tropical analysis as a first estimate of the upper-level flow over a data-void region.

The design of the technique[1] begins from the linearized barotropic vorticity equation:

$$\frac{\partial}{\partial t}\nabla^2\psi + \bar{u}\frac{\partial}{\partial x}\nabla^2\psi - \frac{\partial\psi}{\partial x}\frac{\partial^2\bar{u}}{\partial y^2} + \beta\frac{\partial\psi}{\partial x} = -\left(f - \frac{\partial\bar{u}}{\partial y}\right)B - \bar{B}\nabla^2\psi - D\nabla^2\psi \ , \qquad (1)$$

where

---

[1]The design of the technique is roughly similar to that described by Edwards (1973), although the development is somewhat incomplete and there are also a few errors contained in that paper.

ψ perturbation stream function

$\zeta = \nabla^2\psi$ perturbation relative vorticity

$\bar{u}$ mean zonal wind

f Coriolis parameter

$\beta = \frac{\partial f}{\partial y}$

B perturbation divergence

$\bar{B}$ zonal mean divergence

D a damping coefficient

x,y,t zonal, meridional directions and time, respectively

In Equation (1) the advections due to mean meridional velocity, mean vertical velocity, and the divergent part of the perturbation meridional velocity are all neglected from scale considerations. The term $- D\nabla^2\psi$ is included to represent the strong damping process in the upper troposphere as found by the budget studies. It is also consistent with the in-phase relationship between divergence and vorticity near the outflow level observed by Wallace (1971) because such a relationship requires the magnitude of the damping to be comparable to the divergence forcing (Holton and Colton, 1972). This damping process has not been fully understood. It may be due to strong cumulus transport of low-level vorticity as suggested by Reed and Recker (1971) and Holton and Colton (1972), or it may also be due to some non-linear process. In their study Holton and Colton found that a very strong viscous damping coefficient, $D = 1.5 \times 10^{-5} sec^{-1}$, is necessary in order to compute a realistic seasonal mean stream function field from the observed mean divergence. Other budget studies (for example, see

Williams and Gray) also indicate that D in cloud-cluster areas is considerably larger than that may be expected for the usual large-scale damping time alone.

The corresponding finite-difference equation of (1), expressed by central differencing in both time and space(except that an implicit scheme is used for the damping term due to stability requirement),is

$$
\begin{aligned}
(\nabla^2\psi_{i,j})^{\tau+1} &= \frac{(\nabla^2\psi_{i,j})^{\tau-1}\,[1 - \Delta t\,(\bar{B} + D)]}{[1 + \Delta t\,(\bar{B} + D)]} \\
&+ \frac{2\Delta t}{[1 + \Delta t(\bar{B}+D)]} \cdot \Bigg\{ (-\frac{\bar{u}m}{2d})(\nabla^2\psi_{i+1,j} - \nabla^2\psi_{i-1,j}) \\
&+ (\frac{m}{2d})(\psi_{i+1,j} - \psi_{i-1,j})\,(\bar{u}_{j+1} - 2\bar{u}_j + \bar{u}_{j-1}) \\
&+ (-\frac{\beta d}{2m})\,(\psi_{i+1,j} - \psi_{i-1,j}) - (\frac{Bd^2}{m^2}) \\
&\cdot [f - ((\frac{m}{2d})\,(\bar{u}_{j+1} - \bar{u}_{j-1}))] \Bigg\}^{\tau} , \qquad (2)
\end{aligned}
$$

where

τ index for time step

i,j grid point indices in x and y, respectively

m map factor (equals to unity at 22.5N throughout this study)

d grid interval, same for both x and y (equals to 2.5° at 22.5N throughout the study)

Equation (2) may now be integrated in time over a rectangular region provided that $\bar{u}$, divergence ($\bar{B}$ and B), initial conditions and proper boundary conditions are given. Two neighboring boundary conditions of

ψ are required at both eastern and western boundaries because of the zonal advection term.

Since we will be looking for steady-state solution under forcing, initial condition will not be crucial and is always set to zero for the interior in this study. The specification of $\bar{u}$ posts a problem because it is assumed that we are dealing with a data-void region. However, it may be adequate to use values known from monthly or seasonal mean climatology. The divergence field, which is required as a forcing function for (2),will be given by an equivalent divergence field empirically constructed from digitized satellite brightness data. In the experiments of this model discussed in Section IV, three forcing fields for each day will be tested and results compared with the available NMC flow field: a divergence field kinematically computed from NMC-analyzed winds, an equivalent divergence field from brightness data, and a case of "zero forcing" where $\bar{B} = B = 0$.

The specification of boundary conditions for ψ will depend upon the data available outside of the data-void region. We assume that, in most cases, the data-void region may be selected as a rectangular area or "box" surrounded on all four sides by boxes of arbitrary size within which wind information are adequate (see Figure 1). These data-rich regions may be areas of island groups or edges of continents. If stream functions for each of these data-rich regions can be computed from the wind information, the boundary conditions of the data-void region can be determined because each of the four adjacent data-rich boxes share one common border with the data-void box. There are many methods of computing the stream function from winds for a limited

region. Among them the various versions of Sangster's method, as discussed by Hawkins and Rosenthal (1965), are all quite adequate for our purpose, especially Version III, which was found to give a stream function field closest to the NMC-analyzed field used in our test. We have also tried an iterative version of Sangster's method somewhat similar to that described by Shukla and Saha (1974) but the difference between the iterative and non-iterative version is usually small, and the additional computer time required for iteration is certainly not justified.

Although theoretically a method such as Sangster's must be used in the actual application of our technique, for simplicity the boundary conditions used in the numerous experiments carried out in this study are extracted directly from the available NMC-analyzed stream function field.

III. DATA SOURCES AND PERIOD OF STUDY

In this study we used daily satellite brightness data for July-August 1971 to construct the forcing function for Equation (2). The results are compared to the tropical grid wind data (including stream functions) analyzed by the National Meteorological Center (NMC). The area selected for this study is the tropical western North Pacific, from the equator to 25N and 125E to 175E. This region was selected because of its 11 rawinsonde stations including the Caroline and Marshall Islands, which makes the NMC-analyzed wind data relatively more reliable compared to other areas of the tropics. Figure 2 shows the region and the rawinsonde network.

The digitized cloud brightness and upper-level wind data tapes were provided by the National Center for Atmospheric Research (NCAR). The cloud brightness data, acquired by NCAR from the National Environmental Satellite Service (NESS), are digitized values ranging from zero to ten averaged for 5° x 5° latitude-longitude squares. The daily observation time is approximately 3 PM local time (~ 0000 GMT in the Western Pacific). The upper-level component winds as well as stream function fields at the 200-mb level were acquired by NCAR from the NMC tropical grid analysis. These 200-mb stream function fields will be referred to as the "observed fields" when discussing the experiments of Section IV. The wind and stream function values are given at grid points approximately coinciding with those for the brightness data, and are the results of analyses based on all available rawinsondes, aircraft observations and a few winds deduced from cloud drift as seen

from satellite photographs. In all cases, the 0000 GMT wind data are considered as being closest to the time of satellite observations. All data are interpolated to give values at the 2.5° x 2.5° latitude-longitude grid points used in this study.

Values for divergence were computed kinematically from the analyzed wind and found to be maximum at 200 mb. This is consistent with observational studies conducted by Reed and Recker (1971), Wallace (1971), Nitta (1972), Williams and Gray (1973), and Yanai et al (1973), who all found that a non-divergent level is usually near 300 mb to 400 mb in the tropics and the 200-mb level is the outflow level with maximum divergence. Therefore, only the 200-mb level is tested in the experiments of Section IV.

Before the observed satellite brightness data acquired from NCAR can be used as equivalent divergence forcing in (2), it must be related to the 200-mb divergence field. This is accomplished by a simple scheme. A proportionality factor K is computed by dividing the monthly standard deviation of divergence, σ_{div}, by the monthly standard deviation of brightness, σ_{CB}. The equivalent divergence at each grid point is then computed on a daily basis by the following,

$$(B + \bar{B})_E = K \cdot CB' \qquad (3)$$

where

$(B + \bar{B})_E$ = equivalent divergence

CB' cloud brightness with seasonal mean brightness removed

$K = \frac{\sigma_{div}}{\sigma_{CB}}$ monthly proportionality constant

When this equivalent divergence is used as forcing of (2), it will be referred to as "brightness forcing" in the discussion of the experiments of Section IV.

The divergence and brightness used in this study have been analyzed in a correlation study by Varona (1974). Weak positive correlations between the two fields were found in space, time and also for dominant time scales associated with synoptic disturbances in the period of study, and the correlation coefficients are much lower than those inferred from Wallace's (1971) wave study. This may be due to the quality of the data used, especially the divergence which is kinematically computed from grid point winds analyzed by NMC. We therefore expect that the results of experiments using divergence forcing and brightness forcing will generally be different. It turns out that in a number of cases the brightness forcing actually produces flow fields more closely resembling the observed field than those produced by our divergence data.

IV. RESULTS

A. TEST OF THE MODEL

As mentioned in Section II, our model is similar to that used by Holton and Colton (1972) for the 200-mb seasonal mean vorticity budget study during the northern summer. While Holton and Colton's model used Gaussian elimination after Fourier decomposition in the zonal direction, our model uses a simple initial value technique to find the steady-state solution. Before conducting experiments using brightness forcing, Holton and Colton's problem is redone as a test of our model. Observed seasonal-mean horizontal divergence and zonal wind fields for June-August 1967 obtained from Krishnamurti's (1970) data are used in Equation (2). Observed stream functions are specified at the equator, 45N, 87.5W, and 90W as boundary conditions for this northern tropical global band. A strong damping coefficient, $D = 1.5 \times 10^{-5}$ sec^{-1}, is first used. Holton and Colton found that such a large damping coefficient is necessary for the linearized barotropic vorticity equation to produce a flow field which closely resembles that observed. Figure 3a shows the observed stream function field in this band as deduced by Krishnamurti. Figure 3b shows the stream function field after 72 hours of integration, which is considered the quasi-steady-state solution because further time integration produces only slight changes. It is evident that our model, just as that of Holton and Colton (1972), is capable of reproducing the major circulation features forced by the seasonal mean divergence.

Holton and Colton hypothesized that the strong damping coefficient is necessary because of cumulus-scale vorticity transports in the vertical associated with the monsoonal circulation. However, cumulus activity is strong only over areas with large-scale divergence at the 200-mb level. Thus, the use of a uniformly strong damping coefficient over the entire domain seems inconsistent with the cumulus transport hypothesis. To examine this premise, a second test run of the 200-mb seasonal mean circulation is carried out using two damping coefficients. The strong damping coefficient, $D = 1.5 \times 10^{-5}$ sec^{-1}, is used only in the divergence areas while a weaker damping coefficient, $D = 5 \times 10^{-6}$ sec^{-1}, which is considered to be more realistic for the large-scale flow, is used over convergence areas. The resultant 72-hr solution is shown in Figure 3c and it is evident that the mid-oceanic troughs are too strong. Thus the necessity of including a strong damping coefficient throughout the domain, in effect, suggests that some other viscous process must be present in addition to the possible cumulus damping.

B. EXPERIMENTS WITH BRIGHTNESS FORCING

In the daily diagnostic experiments three types of forcing functions are applied: the "divergence forcing" ($\bar{B} + B$ = the kinematically computed divergence), the "brightness forcing" ($\bar{B} + B$ = the equivalent divergence), and the "zero forcing" ($\bar{B} = B = 0$). Quasi-steady-state solutions after 72 hours of integration are obtained for each day of July and August 1971, but only the results for an eight day representative period are shown here (Figures 4-11). These are the first eight days of August 1971 that have data available, namely 2, 3, 4, 5, 6, 7, 9, and 10 August. For

each day of this period eight computer-plotted diagrams of the perturbation stream function field are shown in the following order:

a. the NMC-analyzed field;

b. the solution for zero-forcing and $D = 1.5 \times 10^{-5}$ sec^{-1};

c. the solution for divergence forcing and $D = 1.5 \times 10^{-5}$ sec^{-1};

d. the solution for brightness forcing and $D = 1.5 \times 10^{-5}$ sec^{-1};

e. the solution for divergence forcing and $D = 5 \times 10^{-6}$ sec^{-1};

f. the solution for brightness forcing and $D = 5 \times 10^{-6}$ sec^{-1};

g. the solution for divergence forcing, $D = 1.5 \times 10^{-5}$ sec^{-1}; and zero boundary conditions ($\psi = 0$ at all boundaries); and

h. the solution for brightness forcing, $D = 1.5 \times 10^{-5}$ sec^{-1}, and zero boundary conditions.

The stream functions for 2 August are shown in Figure 4. The solution obtained from brightness forcing (d) is quite similar to the NMC-analyzed field (a), with some differences in the strength of the major features but generally good agreement between gradients and flow patterns. On the other hand, the results of divergence forcing (c) shows a good correspondence with the NMC-field over the eastern half of the test region but it contains a ficticious trough in the northwestern "high" area. The zero-forcing solution (b) least resembles the NMC field, especially in the north-central sector where the flow displays excessive zonal orientation. As expected the flow fields are too strong for both the divergence and brightness forcing when the damping coefficient is reduced to $D = 5 \times 10^{-6}$ sec^{-1} (e and f). The last two diagrams illustrate the results of the zero boundary condition cases. Here the brightness forcing (h) produces a pattern that better defines the distribution of positive and negative vorticity areas than does the divergence forcing

(g) which is consistent with the results obtained when realistic boundary conditions are given.

Figure 5 shows the stream functions for 3 August. It can be seen that brightness forcing produces a flow field in excellent agreement with the NMC field for the entire region. The field produced by divergence suffers mainly from a fictious trough which is present in the western "high" area. The zero-forcing solution again least resembles the NMC-field. In the eastern central portion the flow is both weak and more zonal, and the cyclonic vorticity also penetrates into the western area although not as strongly as the trough shown in the divergence-forced field. The results for smaller damping are again too strong. This is consistently true for all days tested and we will not make further special reference to it. The value $D = 1.5 \times 10^{-5} sec^{-1}$ is thus considered an appropriate damping coefficient to be used in our model. The results for the zero boundary conditions, as expected, show that the brightness forcing better delineates the regions of negative and positive vorticity than does the divergence forcing.

The results for 4 August, as shown in Figure 6, differ from those obtained on the two previous days. The field produced by brightness forcing does not agree as closely with the NMC field as it did on 2 and 3 August. Both the western and eastern "cells" are somewhat underdeveloped. However, the orientation of the eastern trough is better depicted by this field than by the field produced by the divergence or zero forcing. On the other hand, the western anticyclonic circulation pattern produced by the divergence forcing more closely resembles that of the NMC field. The accurate orientation of the eastern trough

produced by the brightness forcing is clearly depicted in the results for zero boundary conditions. This is seen in Figure 6h, which clearly defines a zone of negative stream function values sloping from the northeast to the southwest. This orientation does not appear in the field produced by the divergence forcing with zero boundary conditions.

Results for 5 August are shown in Figure 7. The major circulation features produced by the brightness forcing do not develop meridionally into the south central portion as those of the NMC field. This particularly true of the southern extension of the -1 contour line of the eastern trough. Somewhat stronger development of this feature is produced by the divergence forcing. This feature is least developed in the solution obtained by zero-forcing, thus on this day the brightness forcing result may still be considered as better than the zero-forcing case. The zero boundary condition results show that although the divergence forcing case defines the orientation of the trough to a certain degree of accuracy, the brightness forcing case depicts the position and strength of the trough much better.

Figure 8 shows that for 6 August brightness forcing produces areas of anticyclonic vorticity over the western half and southeastern corner of the test region, both of which grossly resemble the patterns shown by the NMC-field. However, the northeastern cyclonic circulation is overdeveloped by the brightness forcing. It can be seen that this northeastern quarter of the test area shown in the zero-forcing solution has closer agreement with the NMC-field than does the divergence or the brightness forcings, but the overall resemblance is still best for

the field produced by brightness forcing because of the two anticyclonic areas. When zero boundary conditions are used, the brightness forcing solution is again considerably more accurate in specifying the negative and positive vorticity regions than the results of divergence forcing, although it is not as representative of the major features of the NMC-field as is the case for several previous days.

The results for 7 August are shown in Figure 9. The correspondence between the solution obtained with brightness forcing and the NMC-field appear to be quite poor. However, closer examination reveals that the slope of the -1 contour produced by brightness forcing closely approximates that of the zero contour of the NMC-field, which is orientated NW-SE near the central western portion. Therefore, even though the appearance of the two fields differs considerably, the brightness forcing solution still gives some useful information on the NW-SE flow direction in the central part of the test region, which is not the case for the fields obtained from divergence or zero-forcing. This information on flow direction is also evident in the -1 contour line of the brightness forcing solution with zero boundary conditions.

Figure 10 shows the stream functions for 9 August. On this day all results are considered poor and is clearly a failing case of our model.

The results for 10 August as shown in Figure 11 illustrates another unsuccessful case. The solution obtained from brightness forcing, however, still resembles the NMC-field better than the other forcing solutions. The patterns produced by zero boundary conditions are obviously poor in terms of representing the major circulation features of the NMC-field.

In summary, the above results show that the solutions obtained with the strong damping coefficient, $D = 1.5 \times 10^{-5}$ sec^{-1}, are generally more realistic than those obtained with $D = 5 \times 10^{-6}$ sec^{-1}. In the 8 days discussed, brightness forcing produced stream functions quite similar to the NMC-field on two days (2 and 3 August) and gives useful information on the flow patterns on four days (4, 5, 6 and 10 August). It is also interesting to note that on the failing day of August 9, both the computed divergence and the brightness values are generally small. On this day few values of brightness data in the test area exceed 7, which is the"lowest brightness" day of the 8-day period.

In addition to the solutions presented here, results were obtained for all days in the months of July and August for which data are available. Overall, for approximately 25% of the tested days, brightness forcing produces quite realistic stream functions resembling the NMC-field, and in another 30% of the days it gives some useful information about the flow field. These results suggest that if no wind information is available over a tropical region, a first guess of the 200-mb flow field may be obtained from digitized satellite brightness data using a simple model such as that presented here.

Since the zero forcing results occasionally also give a rough sketch of the flow pattern, even steady-state solutions of the barotropic vorticity equation from boundary information alone may sometimes provide a guess of the flow which is better than nothing. This is especially true when divergence is weak as indicated by low brightness values.

C. EXPERIMENTS WITH FORCING MODIFIED BY TIME INTERPOLATED INFRARED DATA

Since the satellite digitized brightness does not supply direct information on the heights of the cloud clusters observed, the possible existence of low-level high brightness values may distort the upper-level flow pattern obtained from the solution of Equation (2) under brightness forcing. If satellite infrared data (IR) were available for the same time and grid points as satellite cloud brightness data, the values of brightness could be modified according to the height of the cloud tops, which can be inferred from the IR data. This is because the condensation heating at upper levels is obviously related to the vertical extent of cumulus development. If accurate cloud-top temperatures and cloud-top heights can be determined, there may be ways to incorporate this information into the brightness data in order to distinguish the effects due to various vertical developments of cumulus convection. For example, since higher cloud tops are colder, we may assume that by giving higher weights to brightness values coincident with low IR readings the resultant field obtained by brightness forcing of Equation (2) will better approximate the actual field. In this way the high brightness due to solar reflections at the surface would also be completely eliminated as far as the contribution to the divergence at the upper level is concerned.

In 1971, area-averaged, once-daily IR data from the NOAA-1 satellite over the 5° x 5° latitude-longitude grids of the test region are available from NESS for the period 19 April - 10 July. Unfortunately, the observation time is approximately 3 am local time each day (or ~ 1200 GMT in the western Pacific), which is 12 hours different from that of

the brightness data. However, although the life cycle of an individual cumulus element may be ~ 0 (hr), an organized cloud cluster with a scale on the order of the 5° x 5° grid squares usually lasts sveral days or longer. Thus we decided to use the simple average of two consecutive IR observations to approximate the IR information at the brightness observation time. This interpolated data is then used to test the idea of enhancing the brightness forcing. Of course, this interpolation process may introduce large amounts of error, especially since cloud clusters are usually in a transient state with westward movement comparable to the speed of the zonal flow at low levels (Chang, 1970). Nevertheless, this crude representation of the IR data may provide us with some clue as to whether improvement can be reasonably expected in cases when actual IR data is available for use.

The NOAA-1 IR data period overlaps our experimental period only for the first ten days of July 1971; and, due to missing data in the IR tapes, only IR data for 4-5 July and 7-8 July can be used in our averaging procedure. Thus the "0000Z IR fields" are constructed for only two days: 5 July, which is the average of IR data of 4 July and 5 July; and 8 July, which is the average of 7 and 8 July. As done previously for the brightness and NMC data, these averaged IR data are further interpolated to give values at the 2.5° x 2.5° grid points. A quite simple weighting scheme is then used to modify the brightness values by the averaged IR field. This scheme, which is based on the facts that black-body radiation is proportional to the forth power of the temperature while temperature varies almost linearly with height,

is described by the following equation:

$$CB_M = (C - 4\sqrt{IR})\ CB\ , \qquad (4)$$

$$[CB_M = 0 \quad \text{if right hand side of (4) is negative}]$$

where

CB_M	IR modified brightness
CB	original brightness
IR	averaged IR data
C	a parameter

The parameter C is meant to represent the mean sea-surface temperature which may have different values for different latitudes and is the fourth root of a high IR radiation reading at each latitude. For our simple testing, C is determined at each latitude in the following manner:

1) The maximum IR value before averaging is determined for each day (4, 5, 7, and 8 July);

2) The minimum of these four maximum values is taken as the representative sea surface IR radiation; and

3) C is then set to equal to the fourth root of this IR radiation.

The brightness data as modified by (4) is now transformed to the equivalent divergence field by the method described in Section III. Equation (2), with $D = 1.5 \times 10^{-5}\ sec^{-1}$, is then used to obtain 72-hour quasi-steady-state solutions for 5 and 8 July 1971, and compared with the results obtained previously. These are illustrated in Figures 12 and 13 in which the following format is used:

a. the NMC-analyzed field,

b. the solution for divergence forcing,

c. the solution for brightness forcing, and

d. the solution for IR-modified brightness forcing.

Figure 12 shows the results for 5 July 1971. It can be readily seen that the gradients and pattern of the northwestern "high" area produced by the brightness forcing is improved by the IR modification and resembles the NMC-field better. On 8 July 1971, which is shown in Figure 13, significant improvement can again be found. In the center and center-east sections, the gradients produced by the IR modification is evidently closer to those of the NMC field than the unmodified forcing result. Thus our simple test suggests that there is great potential for the use of IR data to enhance the digitized brightness. The prospect in the future should be quite bright when concurrently-available IR data are used with brightness data, and when a better modification method is designed to replace (4).

V. SUMMARY AND CONCLUSION

In this study we proposed a simple objective technique which may be used to obtain large-scale flow information over tropical regions where wind reports are sparse or void. The technique is basically a diagnostic model consisting of a linearized barotropic vorticity equation. Primary assumptions of the technique are: 1) satellite brightness data is positively correlated with horizontal divergence; 2) tropical flow is quasi-barotropic and quasi-non-divergent. Partial observational justification for the first assumption has been provided by Wallace (1971), and the second one is accepted from the results of scale analysis (Holton, 1972). Another assumption used in the present technique is that, at levels where divergence is strong, the rotational part of the large-scale flow is largely determined by the balance between divergence forcing, strong viscous damping and advection. This "steady state" assumption is based on the results of various budget studies (for example, Reed and Recker, 1971; and Williams and Gray, 1973).

The technique employs an initial-value approach to a finite-difference form of the linearized barotropic vorticity equation applied at a strong-divergence level (usually near 200-mb). The strong damping process is parameterized using a damping coefficient. Three types of information are needed to obtain the quasi-steady-state solution of this equation, which is considered to be an estimate of the actual flow field. These are, 1) appropriate boundary conditions, 2) the mean

zonal flow, and 3) a divergence forcing function. It is suggested that Sangster's (1960) method for computing stream functions from winds can be used for obtaining boundary conditions from the wind reports in areas surrounding the data-void region. The mean zonal winds are supposedly available from monthly-mean climatology. The forcing function is an equivalent divergence field empirically constructed from the digitized satellite brightness data.

The model is tested at the 200-mb level for each day of July and August 1971, over a region of the western North Pacific bounded by the equator, 25N, 125E, and 175E. The data base is formed by the daily digitized cloud brightness data from NESS, and the analyzed upper-level winds and stream functions from NMC. Both of these are available at 5° x 5° latitude-longitude grid points and are packed into computer tapes by NCAR. A daily divergence field is computed kinematically over the test region using the analyzed wind field based on 0000 GMT wind observations. Comparisons are then made among the 72-hour quasi-steady-state solutions of the model as it responds to forcing by the kinematic divergence field (divergence forcing), an equivalent divergence field constructed from brightness data (brightness forcing), and a case in which no forcing is applied (zero forcing). Results for a representative period, the first 8 days of August with available data, are presented and discussed.

In approximately 25% of the days of the entire two-month period of experiments, the solutions produced from brightness forcing are found to accurately reproduce the major features of the perturbation stream

function fields analyzed by NMC. In another 30% of the days these solutions provide some valuable information about the flow patterns which would be difficult to obtain from boundary information alone. In some cases, especially when the divergence and brightness values are low, the solutions of zero forcing also resemble the NMC field to a certain degree. The results of these experiments thus suggest that for data-sparse tropical regions, this model may be useful in obtaining a first estimate of the actual large-scale flow field. This estimate may then be used to supplement whatever other information is available to improve the analysis in these regions.

The technique proposed here may be improved in the future when better data and better understanding of the various physical processes of the large-scale tropical flow are available. For example, it is shown in two cases of this study that even with crude representations of the satellite IR data, the brightness forcing can be enhanced to produce more realistic flow patterns. Better understanding of the physical processes should enable us to improve the parameterization of the strong damping and the handling of the local time change term. Both better data and knowledge of the physical processes would also facilitate our understanding of the relationships between satellite cloud data, condensation heating and the resultant divergence and vertical motion. Therefore, the scheme for specifying the forcing field from the various satellite data may also be greatly improved.

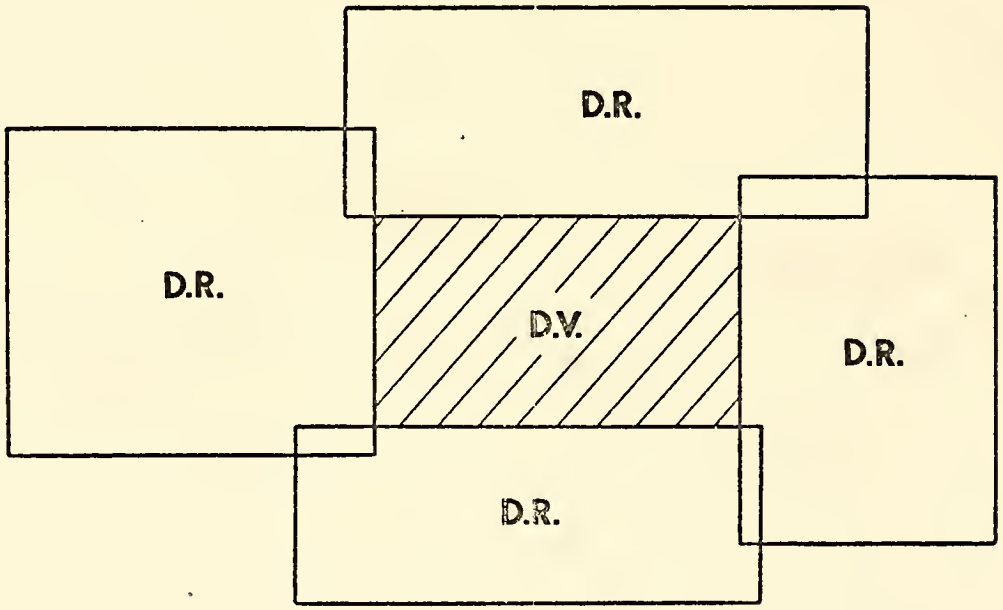

Figure 1. Schematic diagram for computing boundary conditions of the data-void (DV) region from wind information of the surrounding data-rich (DR) regions.

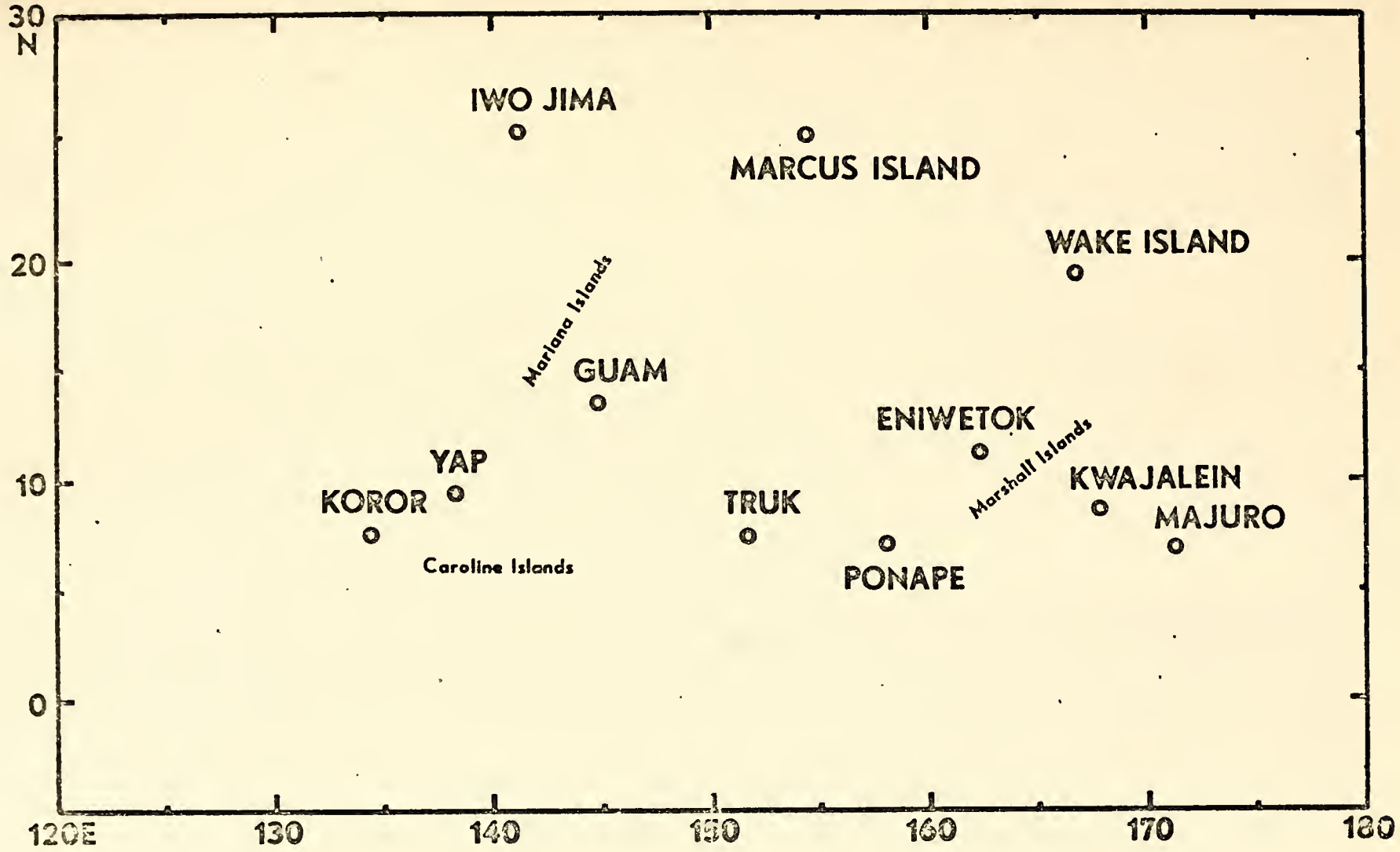

Figure 2. Region of study and observational network.

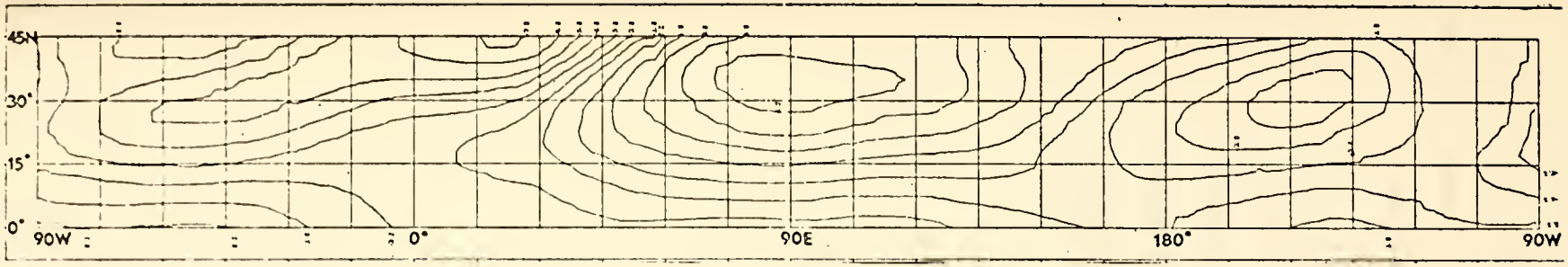

(a) Based on Krishnamurti's mean data

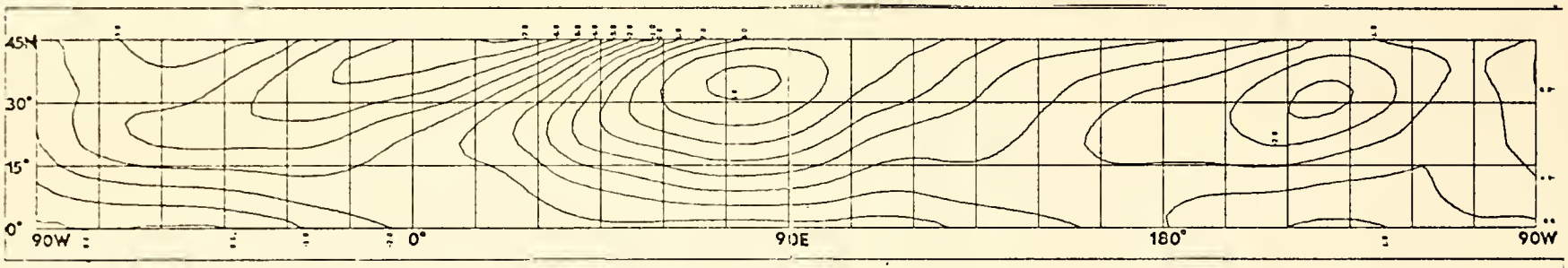

(b) 72-hour basic model solution with $D = 1.5 \times 10^{-5}$ sec^{-1}

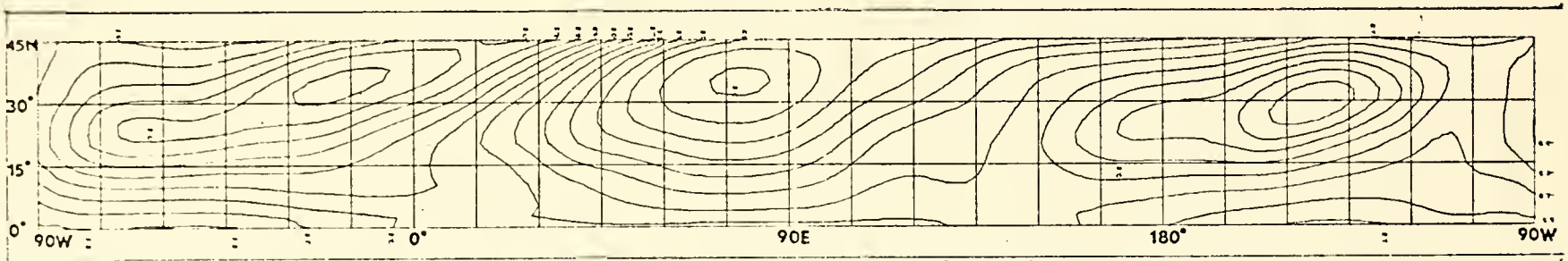

(c) Same as (b) for divergence areas but with $D = 5 \times 10^{-6}$ sec^{-1} for convergence areas

Figure 3. Seasonal mean-flow at 200-mb for June-August 1967. Contour stream function interval is 5×10^{6} m^2 sec^{-1}.

Figure 4. Perturbation stream functions at 200-mb for 2 August 1971 (contour interval is 5×10^{6} m^2 sec^{-1}). Fields shown are:

a. The NMC-analyzed field; and the 72-hr solutions resulting from

b. zero forcing with $D = 1.5 \times 10^{-5}$ sec^{-1} ,

c. divergence forcing with $D = 1.5 \times 10^{-5}$ sec^{-1} ,

d. brightness forcing with $D = 1.5 \times 10^{-5}$ sec^{-1} ,

e. divergence forcing with $D = 5 \times 10^{-6}$ sec^{-1} ,

f. brightness forcing with $D = 5 \times 10^{-6}$ sec^{-1} ,

g. divergence forcing with zero boundary conditions and $D = 1.5 \times 10^{-5}$ sec^{-1} , and

h. brightness forcing with zero boundary conditions and $D = 1.5 \times 10^{-5}$ sec^{-1} .

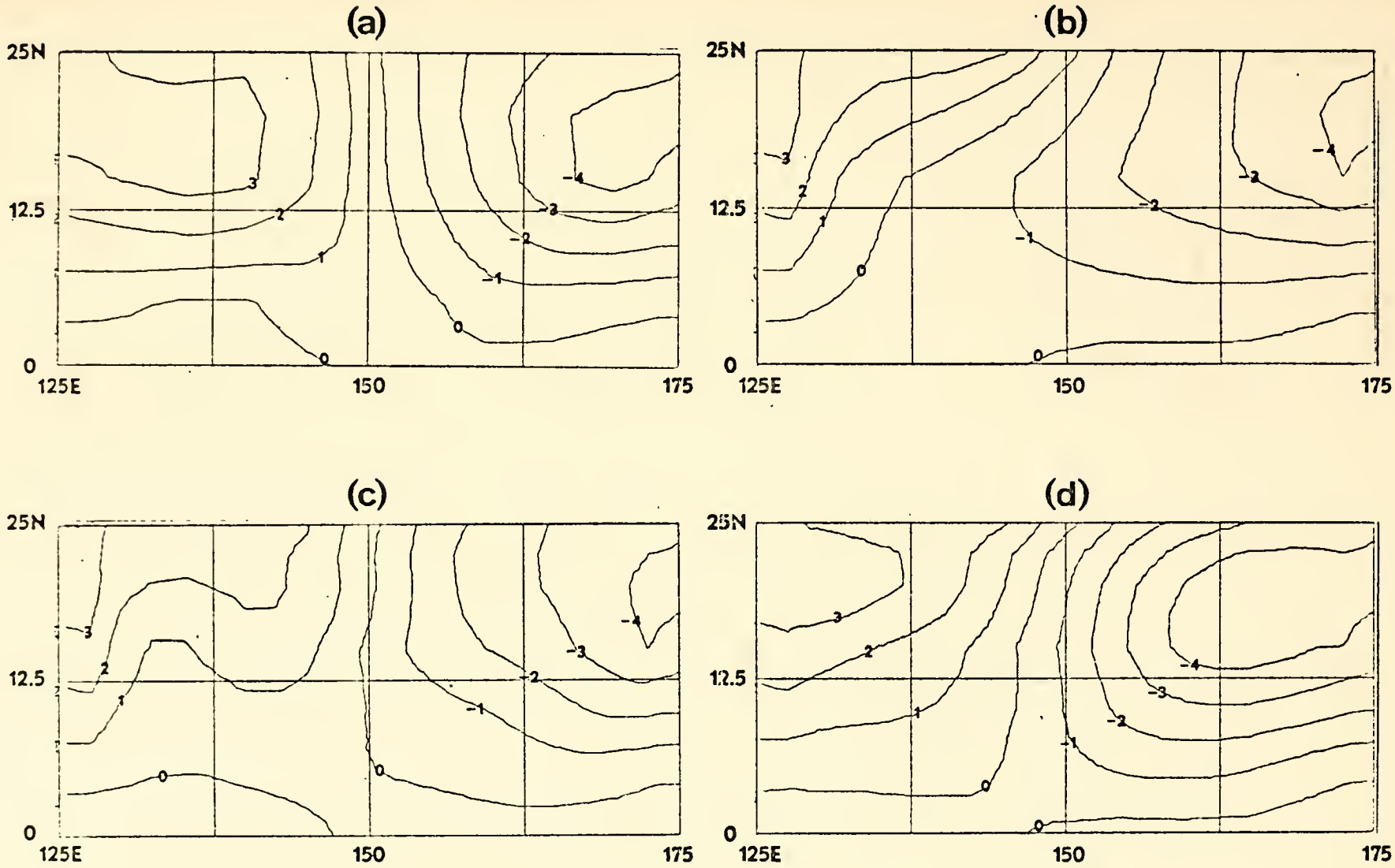

Figure 4. (continued) 2 August 1971.

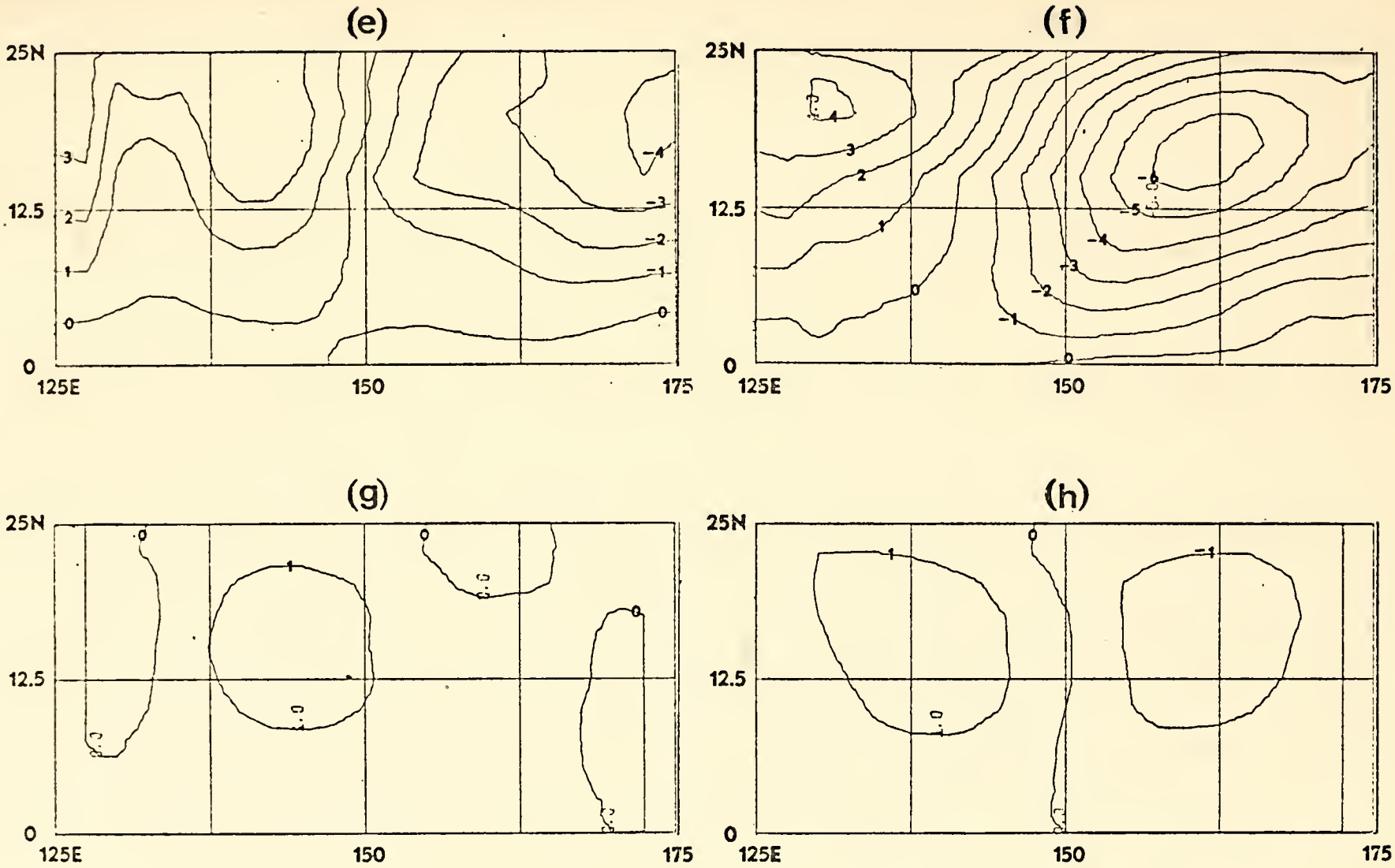

Figure 4. (continued) 2 August 1971

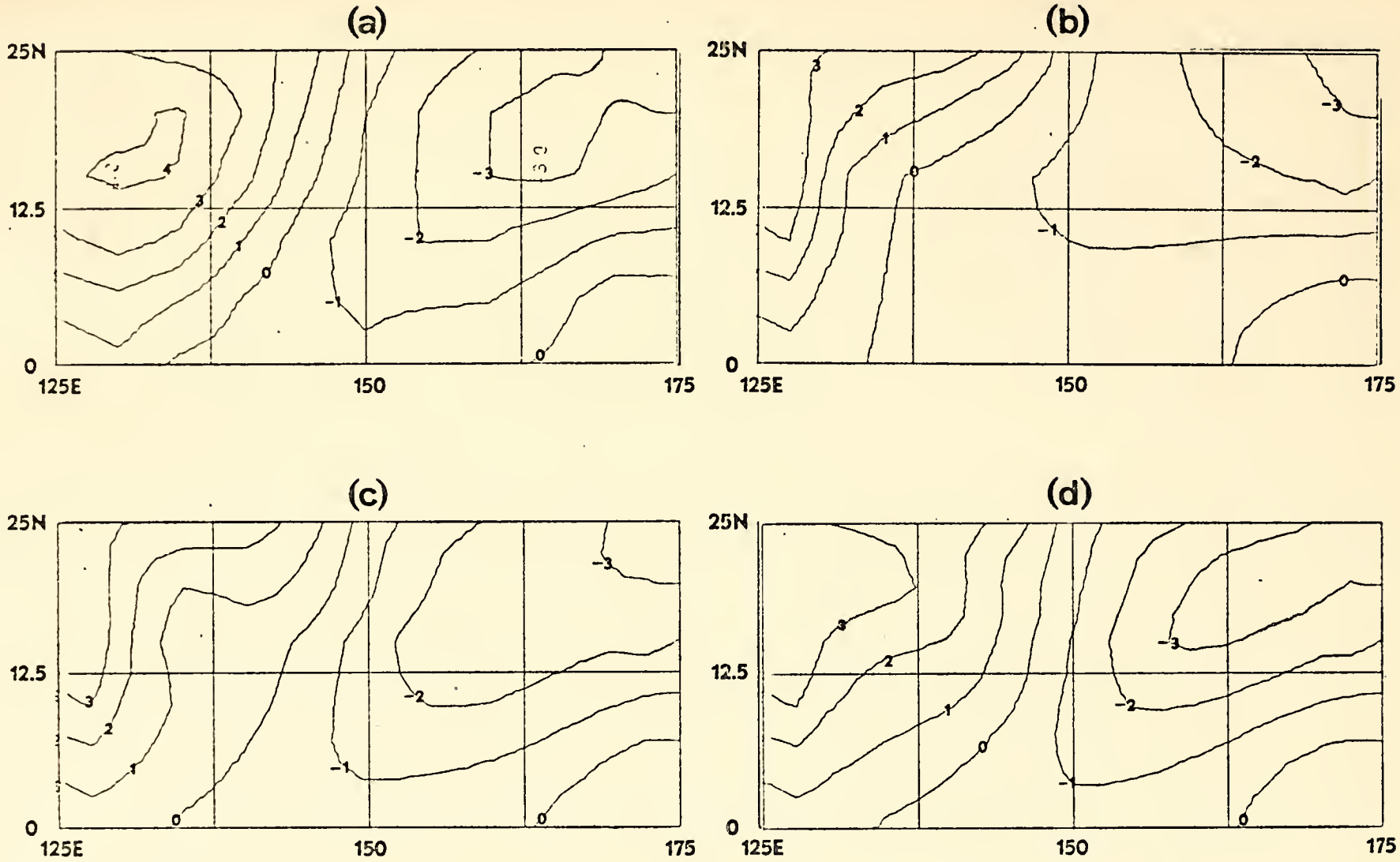

Figure 5. Same as Figure 4 except for 3 August 1971.

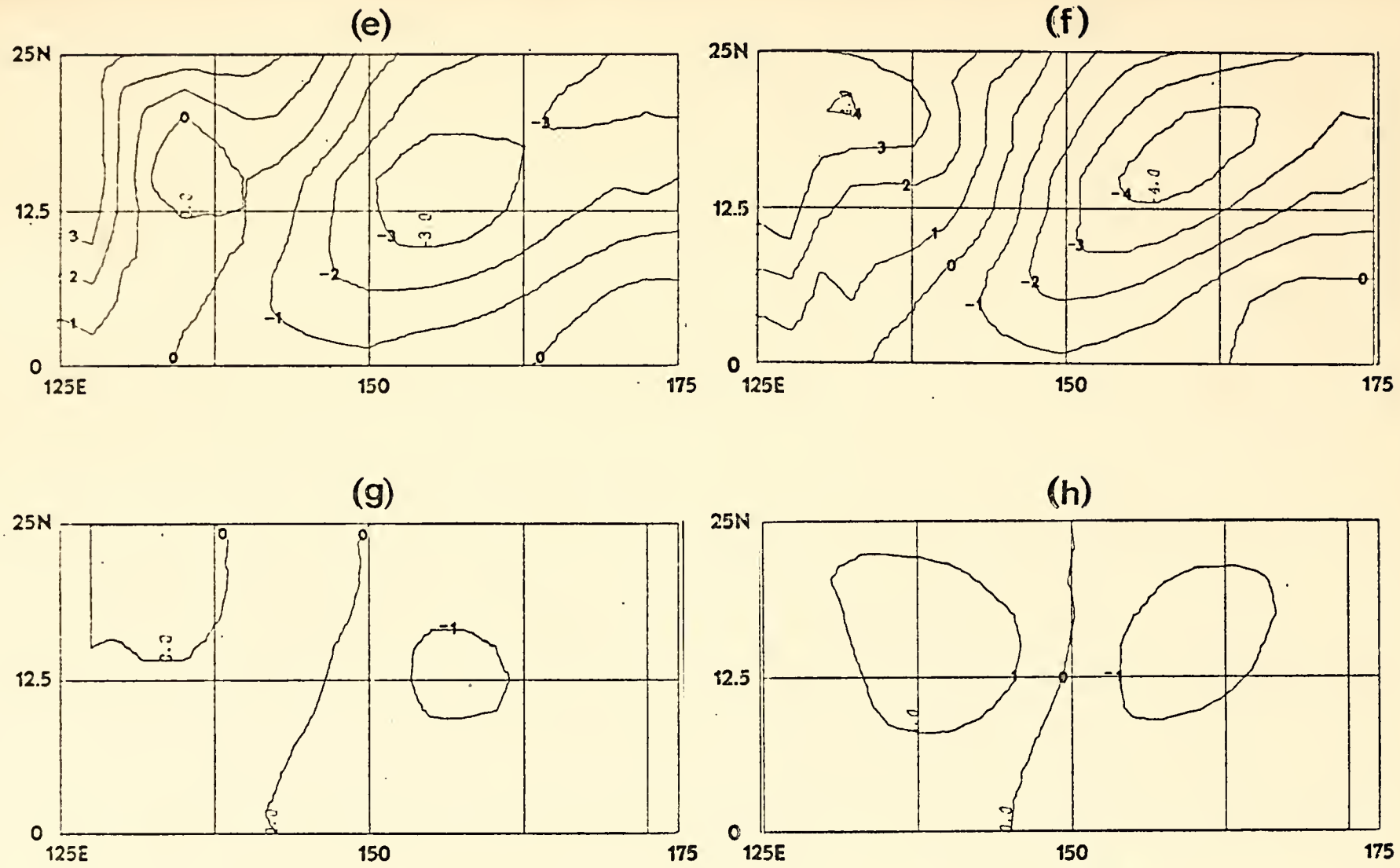

Figure 5. (continued) 3 August 1971.

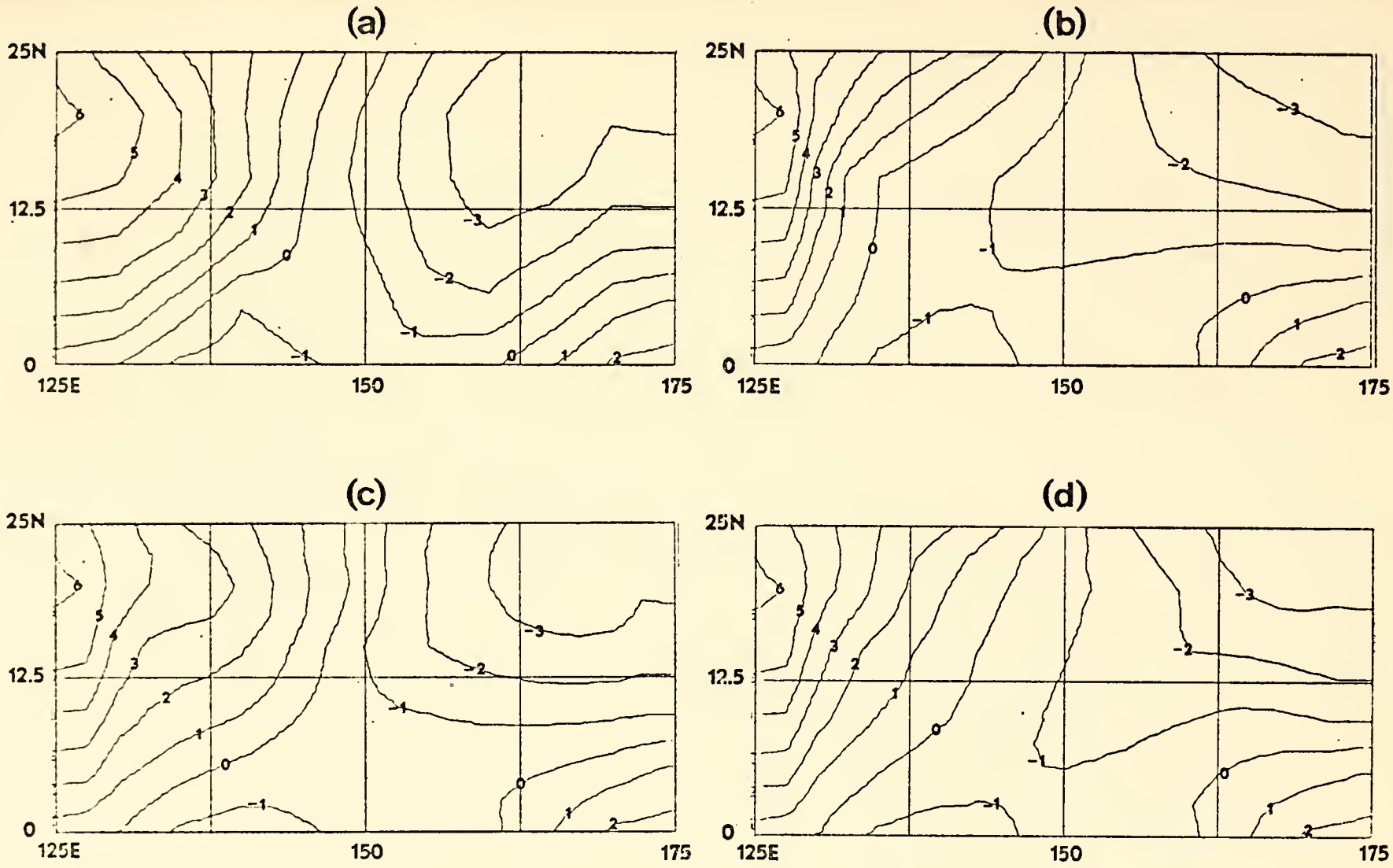

Figure 6. Same as Figure 4 except for 4 August 1971.

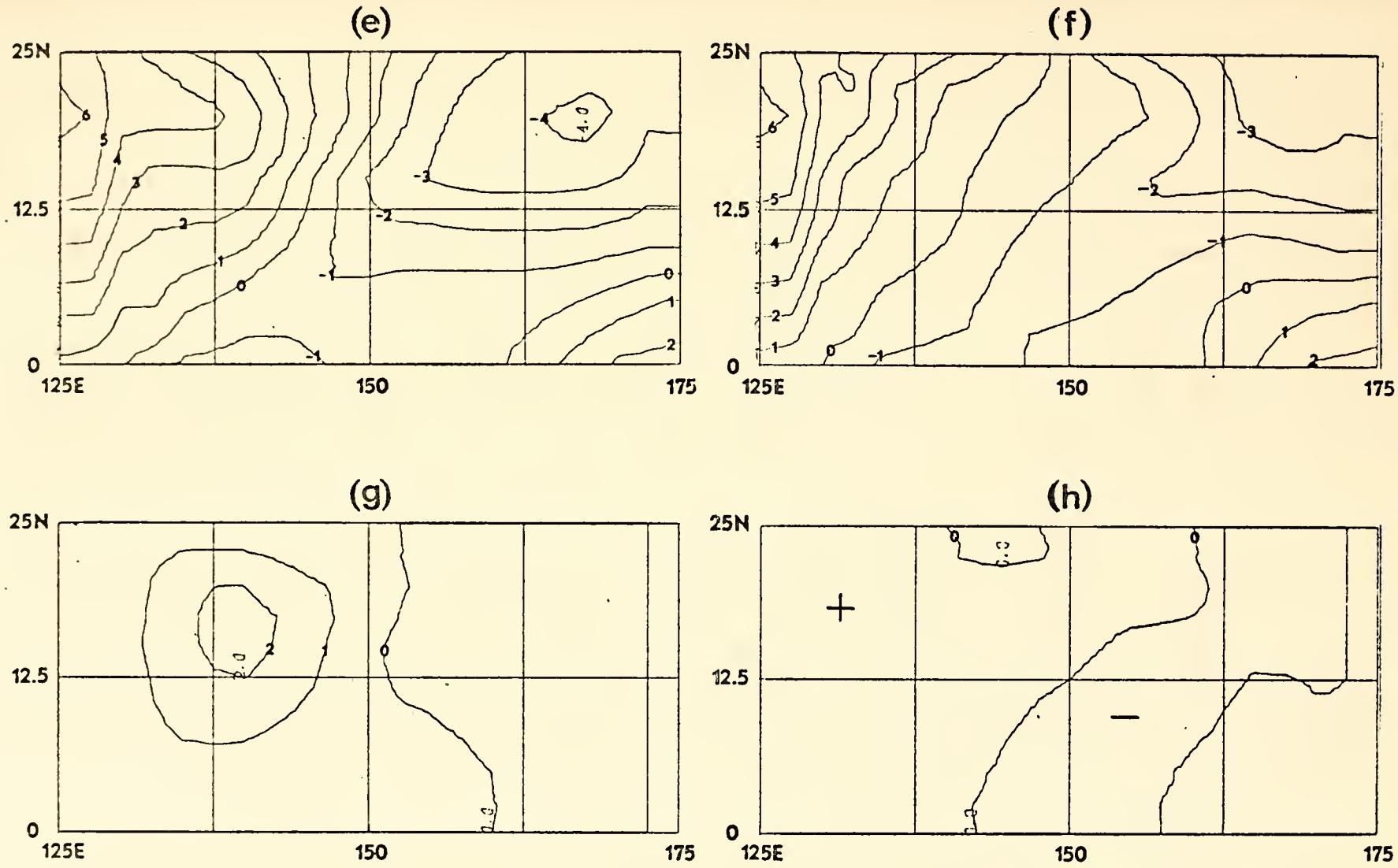

Figure 6. (continued) 4 August 1971.

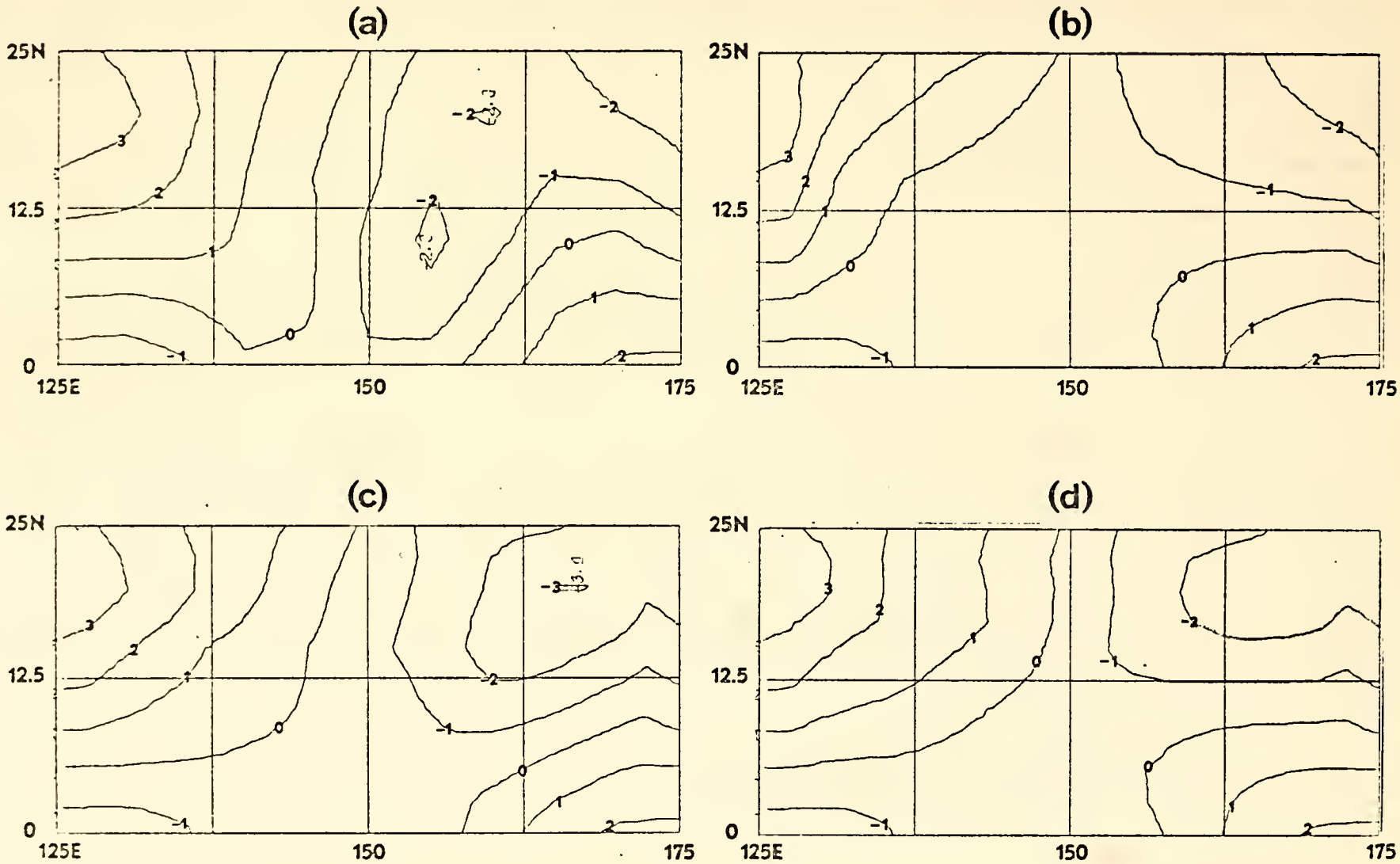

Figure 7. Same as Figure 4 except for 5 August 1971.

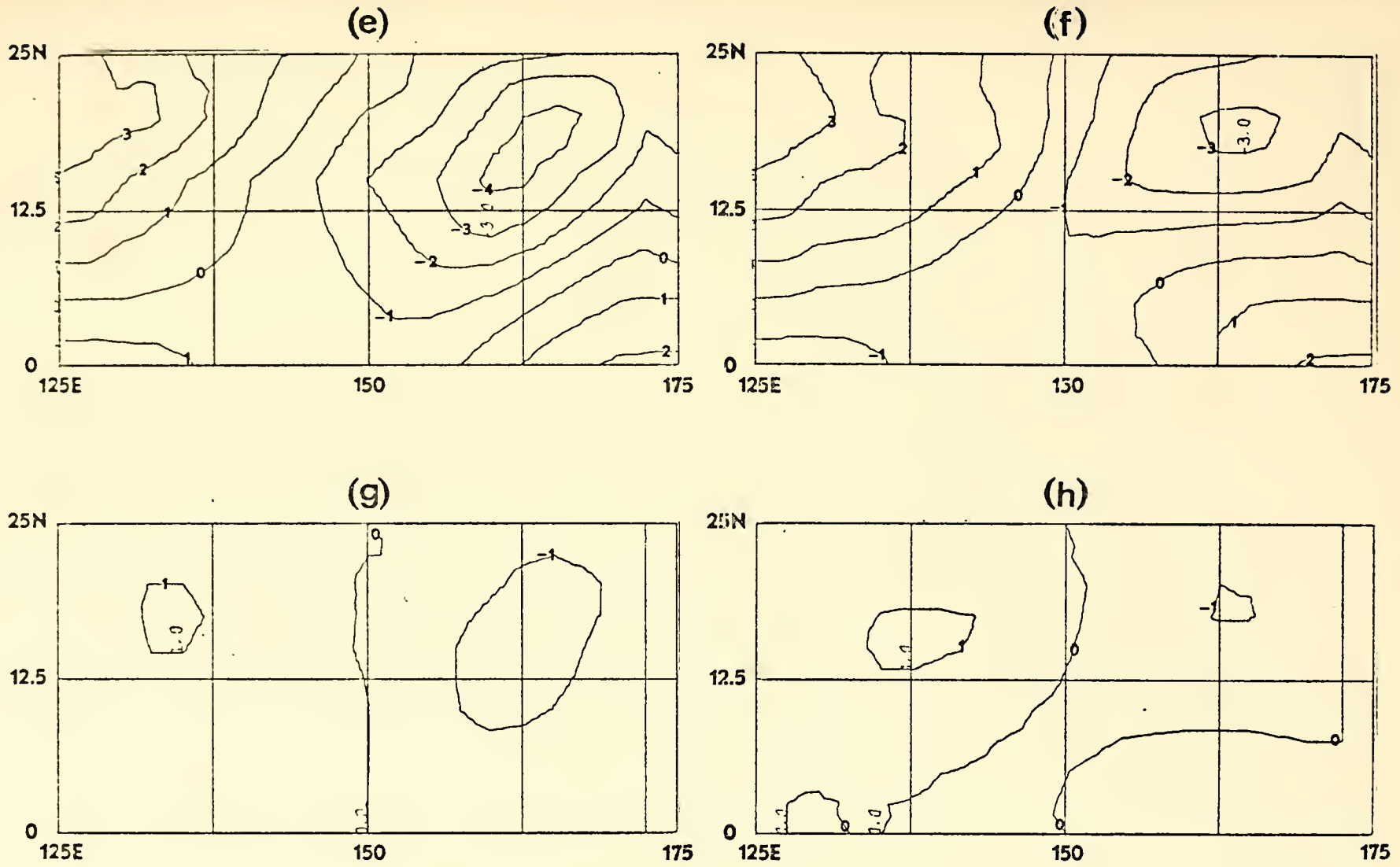

Figure 7. (continued) 5 August 1971.

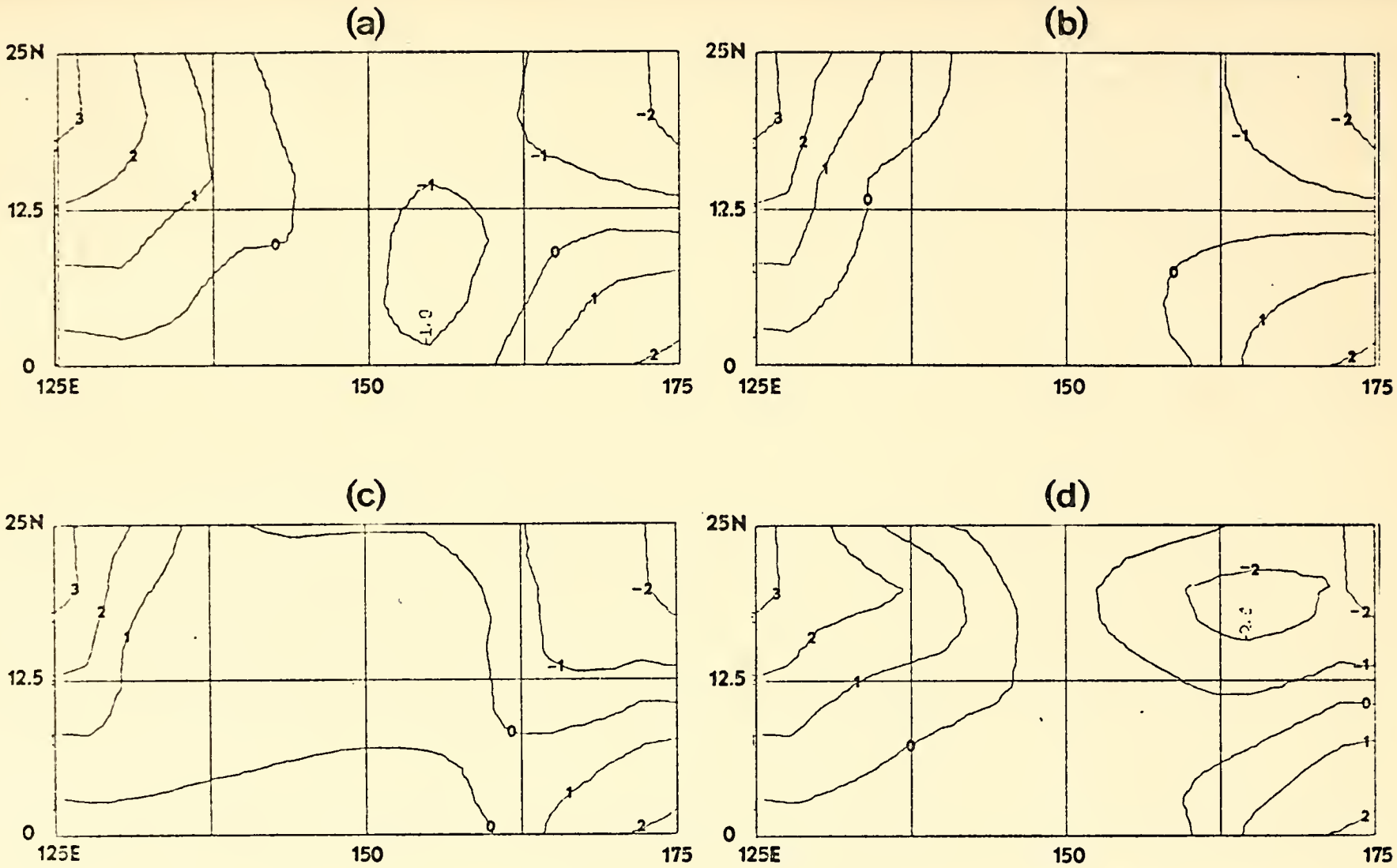

Figure 8. Same as Figure 4 except for 6 August 1971.

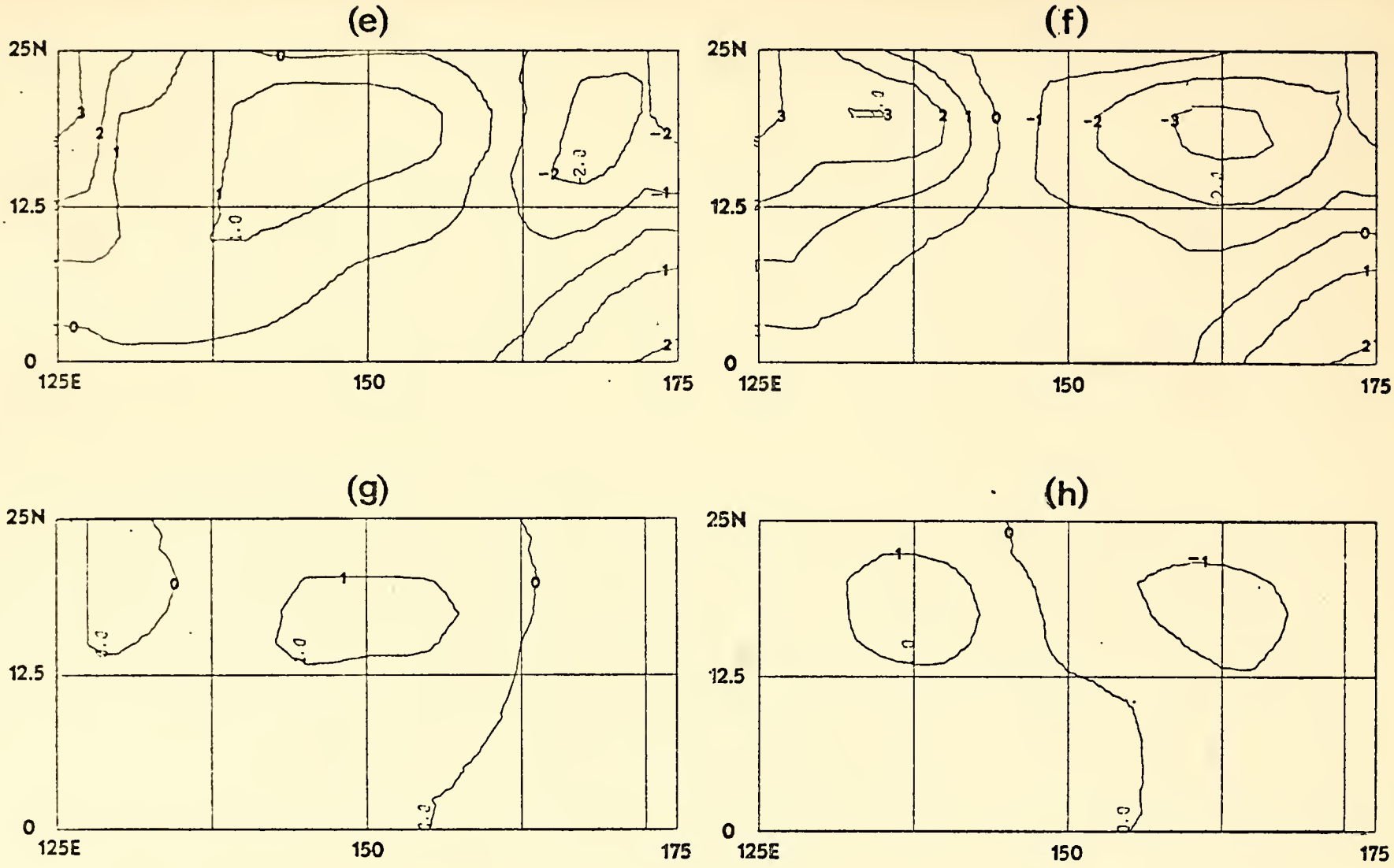

Figure 8. (continued) 6 August 1971.

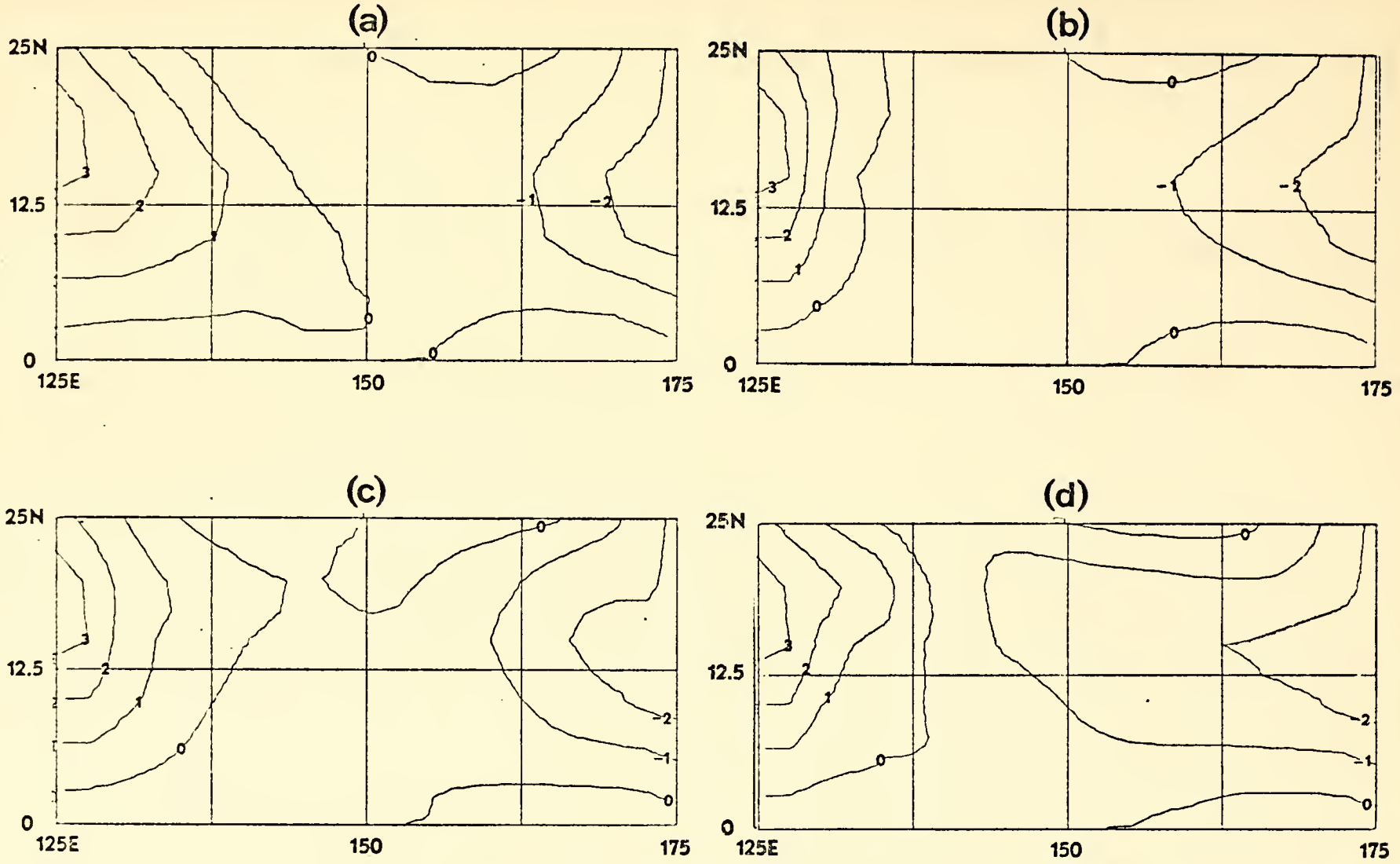

Figure 9. Same as Figure 4 except for 7 August 1971.

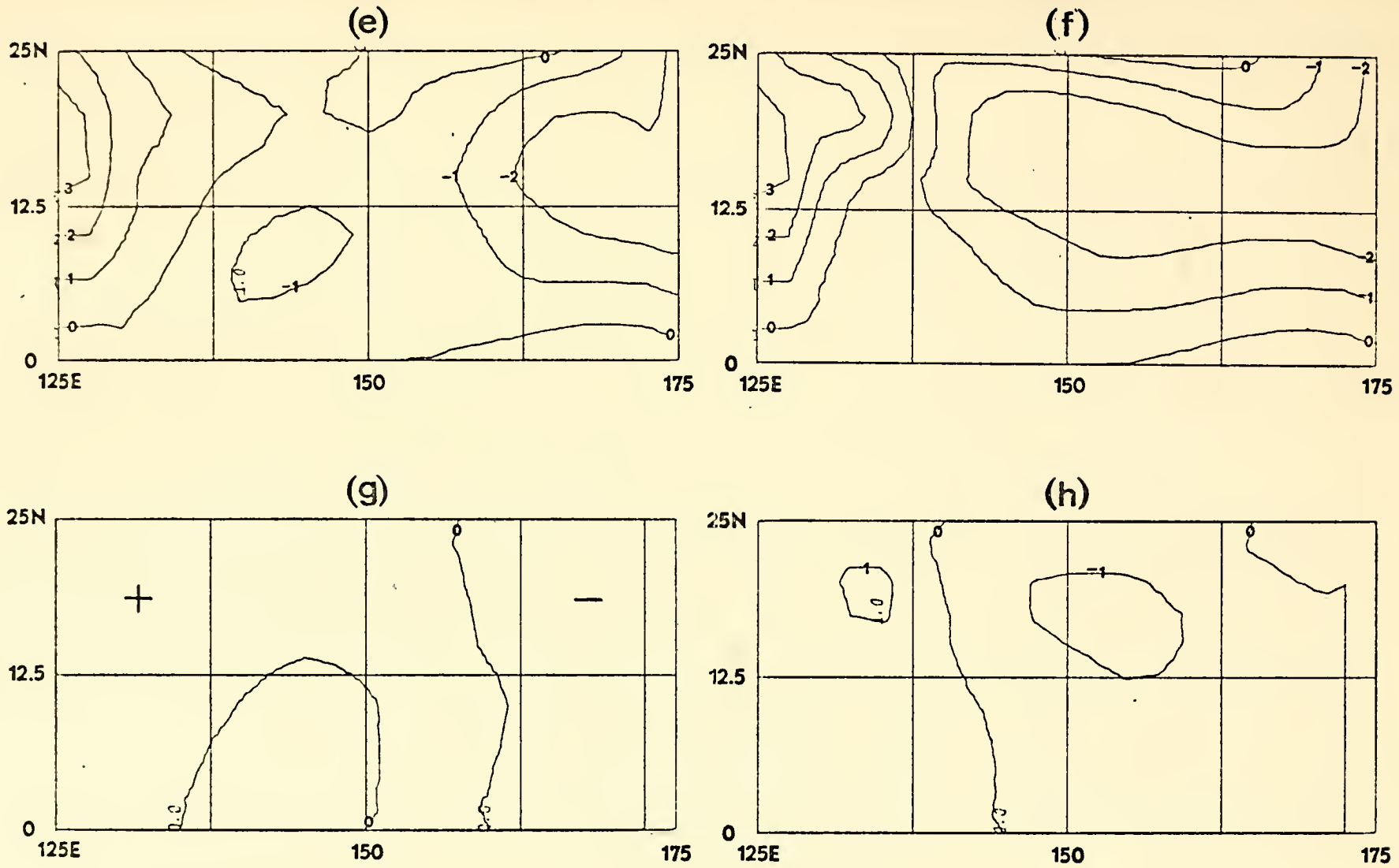

Figure 9. (continued) 7 August 1971.

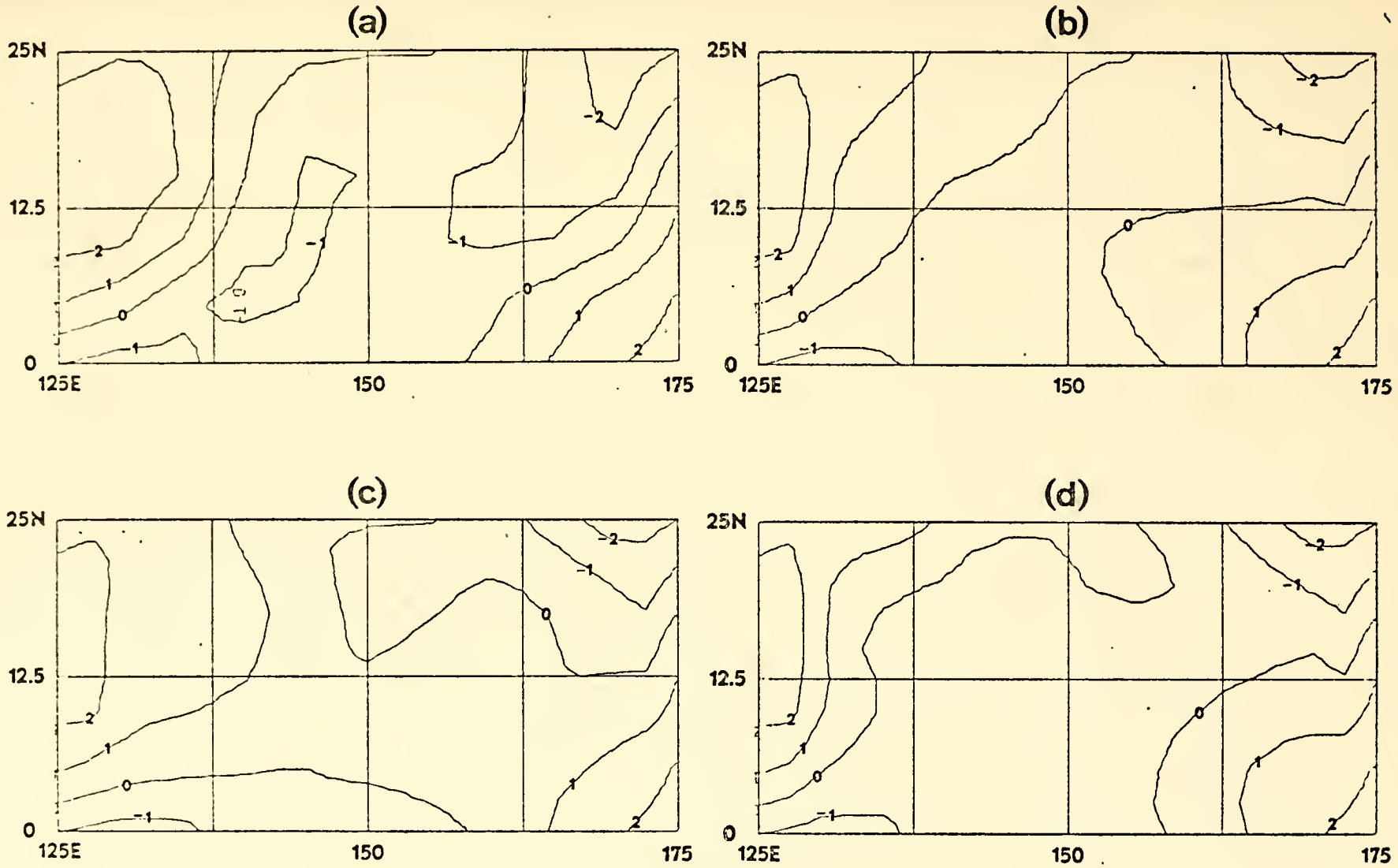

Figure 10. Same as Figure 4 excpet for 9 August 1971.

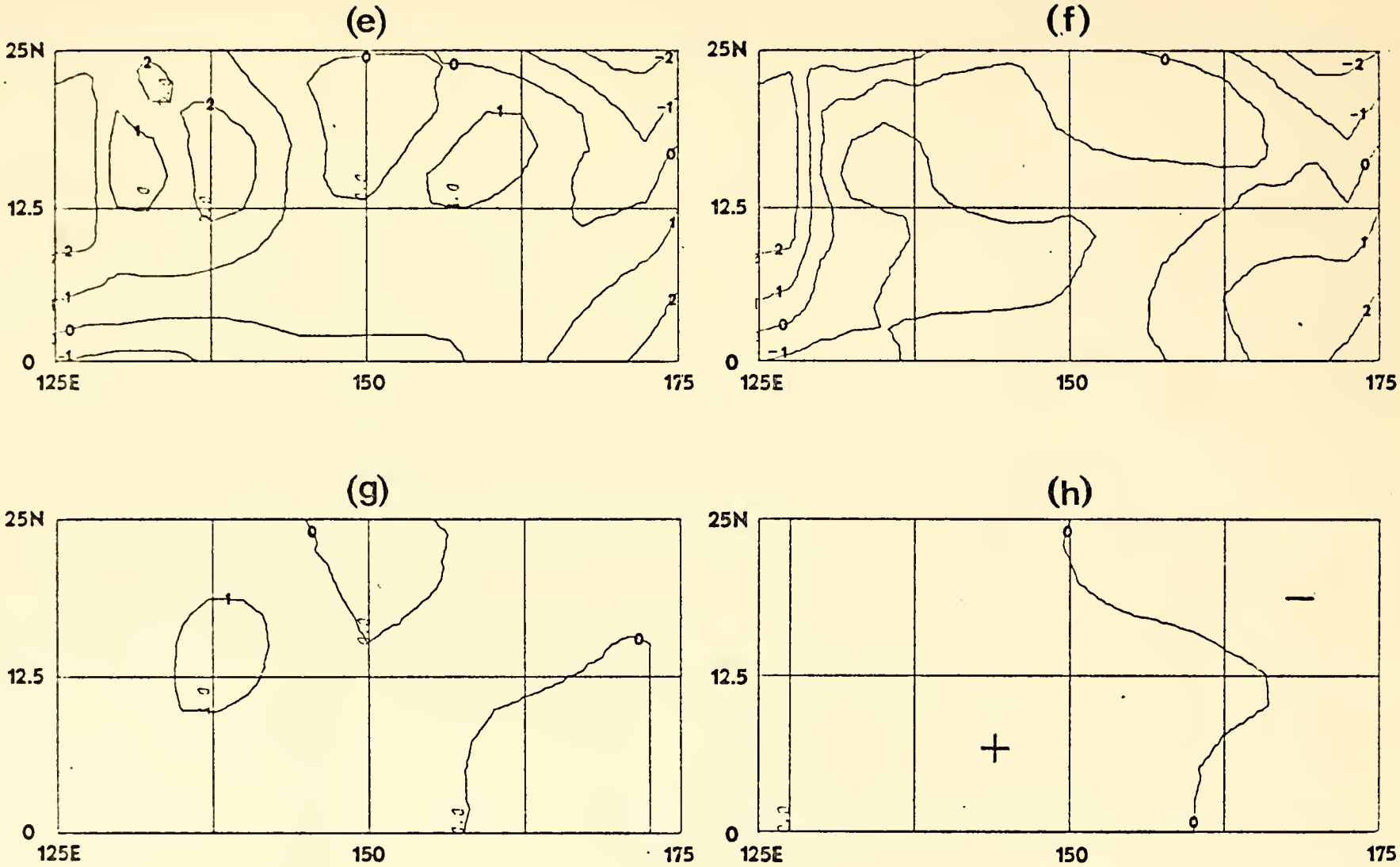

Figure 10. (continued) 9 August 1971.

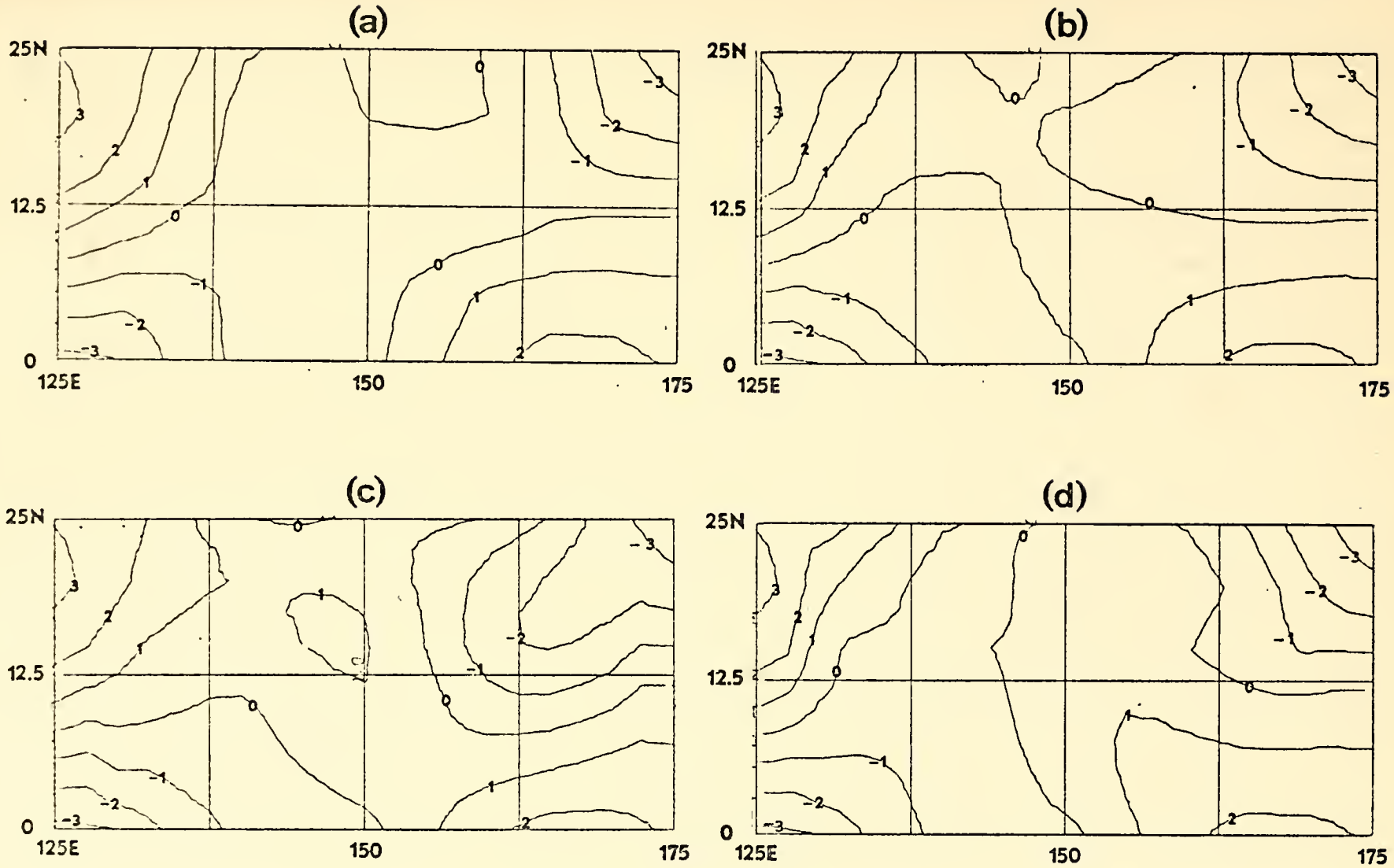

Figure 11. Same as Figure 4 except for 10 August 1971.

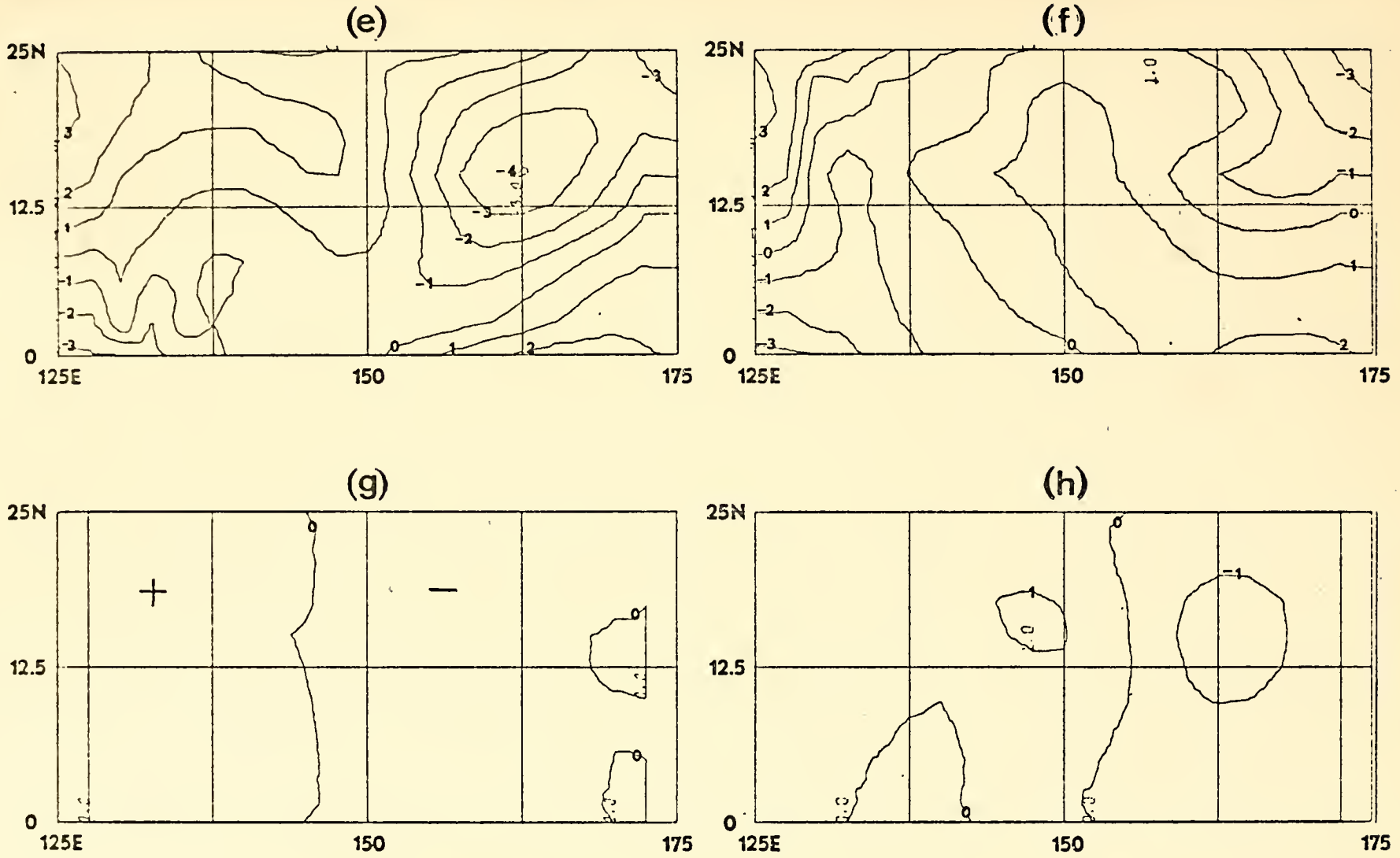

Figure 11. (continued) 10 August 1971.

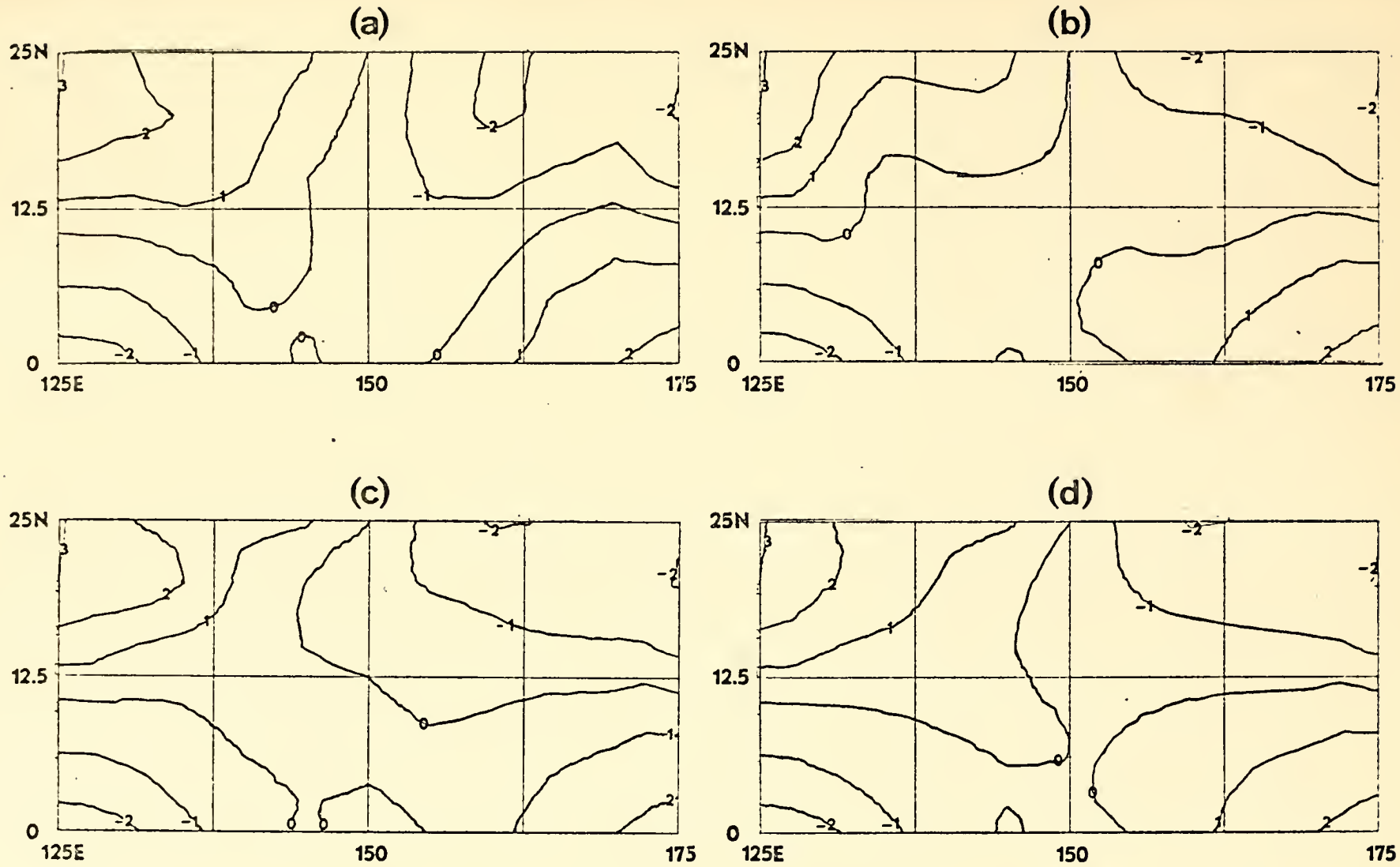

Figure 12. Perturbation stream function at 200 mb for 5 July 1971 (contour interval is 5 x 10^6 $m^2 sec^{-1}$). Fields shown are: a) the NMC-analyzed field; and the 72-hr solutions with D = 1.5 x 10^{-5} sec^{-1} resulting from b) divergence forcing, c) brightness forcing, and d) IR-modified brightness forcing.

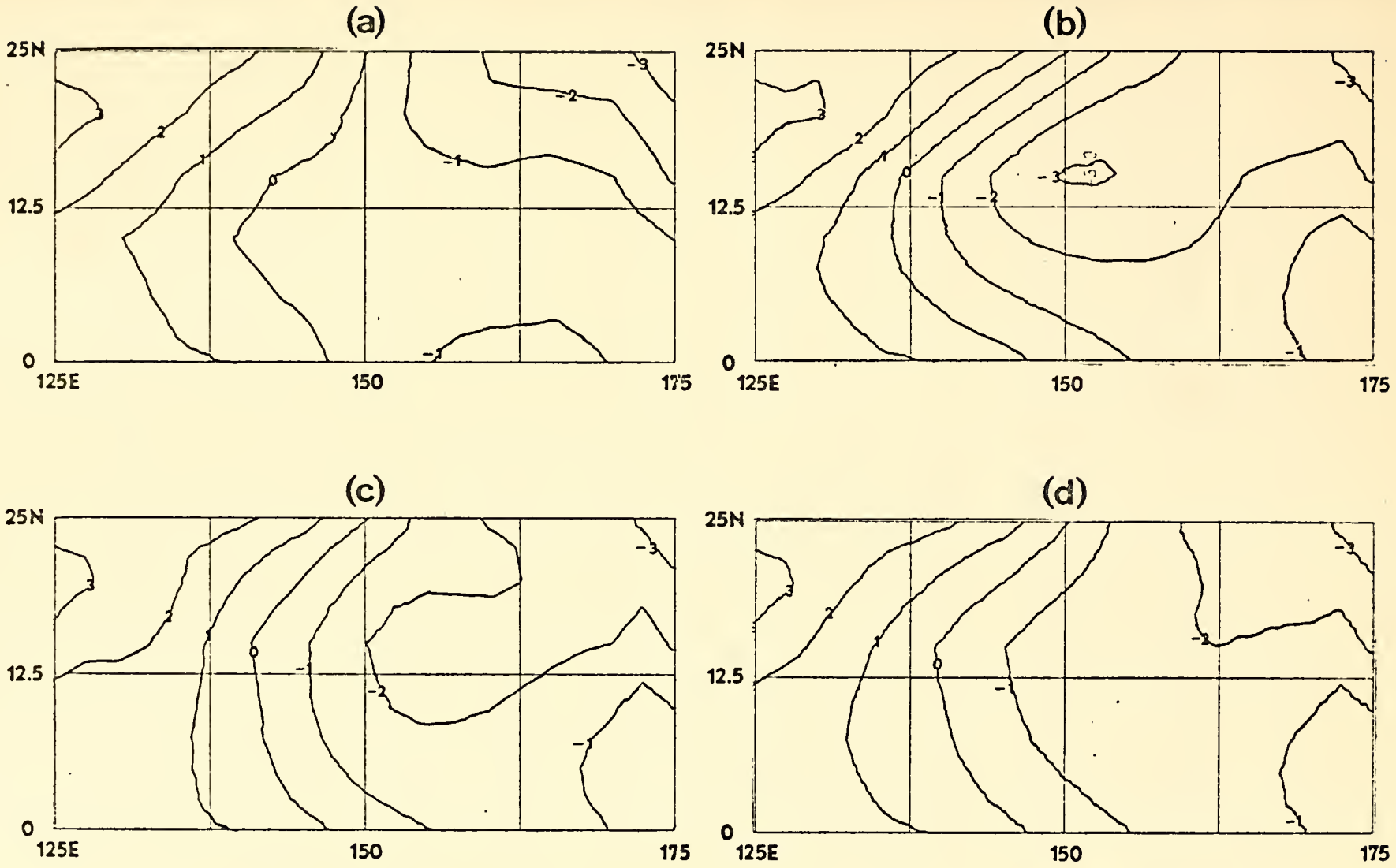

Figure 13. Same as Figure 12 except for 8 July 1971.

LIST OF REFERENCES

1. Chang, C.-P., 1970: "Westward propagating cloud patterns in the tropical Pacific as seen from time-composite satellite photographs." J. Atmos. Sci., 27, 133-138.

2. Edwards, B. E., 1973: A case study on the use of digitized cloud brightness data to represent large-scale convection in the tropics, M. S. Thesis, Department of Meteorology, Naval Postgraduate School, Monterey, California, 50 pp.

3. Gruber, A., 1974: "Wave number-frequency spectra of satellite measured brightness in the tropics." J. Atmos. Sci., 31, in press.

4. Hawkins, H. F., and S. L. Rosenthal, 1965: "On the computation of stream functions from the wind field." Mon. Wea. Rev., 93, 245-252.

5. Hayashi, Y., 1974: "Spectral analysis of tropical disturbances appearing in a GFDL general circulation model." J. Atmos. Sci., 31, 180-218.

6. Holton, J. R., 1972: An introduction to dynamic meteorology. New York, Academic Press, 319 pp.

7. _____, and D. E. Colton, 1972: "A diagnostic study of the vorticity balance at 200 mb in the tropics during the northern summer." J. Atmos. Sci., 29, 1124-1128.

8. Martin, D. W., and W. D. Scherer, 1973: "Review of satellite rainfall estimation methods." Bull. Amer. Meteor. Soc., 54, 661-674.

9. Murakami, T., and F. P. Ho, 1972: "Spectrum analysis of cloudiness over the northern Pacific." J. Meteor. Soc. Japan, 50, 285-300.

10. Nitta, T., 1972: "Structure of wave disturbances over the Marshall Islands during the years of 1956 and 1958." J. Meteor. Soc. Japan, 50, 85-103.

11. Reed, R. J., and R. H. Johnson, 1974: Diagnosis of cloud population properties in tropical easterly waves. Preprints, International Tropical Meteorology Meeting, Nairobi, 50-55.

12. _____, and E. E. Recker, 1971: "Structure and properties of synoptic scale wave disturbances in the equatorial western Pacific." J. Atmos. Sci., 28, 1117-1133.

13. Shukla, J., and K. R. Saha, 1974: "Computation of non-divergent stream function and irrotational velocity potential from the observed winds." Mon. Wea. Rev., 102, 419-425.

14. Varona, E., 1974: A comparative study of digitized brightness and 200-mb divergence in the tropical western North Pacific. M.S. Thesis, Department of Meteorology, Naval Postgraduate School, Monterey, California, 49 pp.

15. Wallace, J. M., 1970: Time-longitude sections of tropical cloudiness (Dec. 1966 - Nov. 1967). ESSA Tech. Report, NESC 56, Washington, D. C., 37 pp.

16. _____, 1971: "Spectral studies of tropospheric wave disturbances in the tropical western Pacific." Rev. Geophys. Space Phys., 9, 557-612.

17. Williams, K. T., and W. M. Gray, 1973: "Statistical analysis of satellite-observed tradewind cloud clusters in the western North Pacific." Tellus, 25, 313-336.

18. Yanai, M., S. Esbensen, and J.-H. Chu, 1973: "Determination of bulk properties of tropical cloud clusters from large-scale heat and moisture budgets." J. Atmos. Sci., 30, 611-627.

INITIAL DISTRIBUTION LIST

		No. Copies
1.	Defense Documentation Center Cameron Station Alexandria, Virginia 22314	2
2.	Library, Code 0212 Naval Postgraduate School Monterey, California 93940	2
3.	Professor C.-P. Chang, Code 51Cj Department of Meteorology Naval Postgraduate School Monterey, California 93940	7
4.	Lieutenant Frederick T. Jacobs USN 1488 Hill Avenue Cincinnati, Ohio 45231	2
5.	Professor G. J. Haltiner, Code 51Ha Department of Meteorology Naval Postgraduate School Monterey, California 93940	1
6.	Department of Meteorology, Code 51 Naval Postgraduate School Monterey, California 93940	2
7.	Commander, Naval Weather Service Command Naval Weather Service Headquarters Washington Navy Yard Washington, D. C. 20374	1
8.	Naval Oceanographic Office Library (Code 3330) Washington, D. C. 20373	1
9.	Fleet Numerical Weather Central Naval Postgraduate School Monterey, California 93940	1
10.	Environmental Prediction Research Facility Naval Postgraduate School Monterey, California 93940	1

11. Professor F. L. Martin, Code 51Mr — 1
Department of Meteorology
Naval Postgraduate School
Monterey, California 93940

12. Professor R. T. Williams, Code 51Wu — 1
Department of Meteorology
Naval Postgraduate School
Monterey, California 93940

Thesis
J234
c.1

155177

Jacobs
An objective for estimating large-scale flow pattern in the tropical upper troposphere from digitized cloud brightness data.